iScience

CellPress

Article

Mycobacterium tuberculosis Mannose-Capped Lipoarabinomannan Induces IL-10-Producing B Cells and Hinders CD4^{+}Th1 Immunity

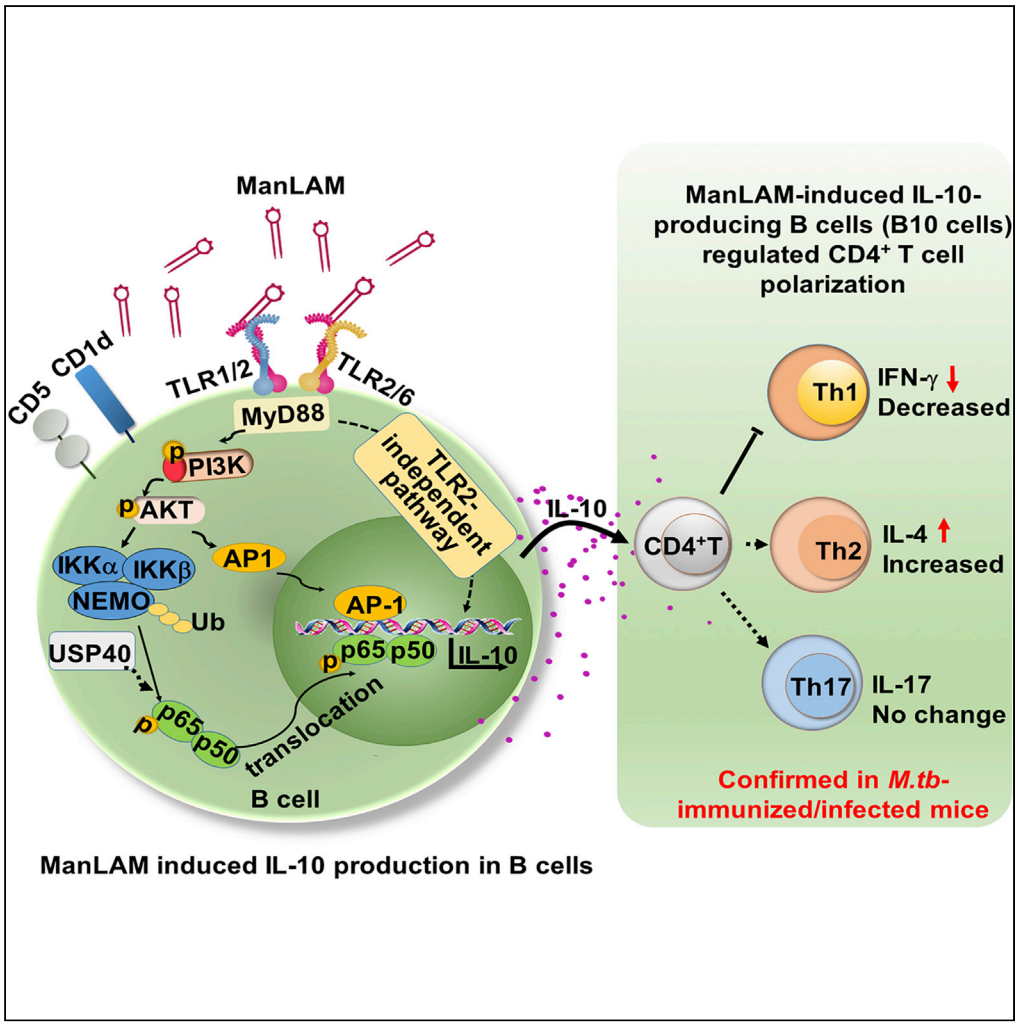

Chunhui Yuan, Zi-Lu Qu, Xiao-Lei Tang, ..., Chun Huang, Qin Pan, Xiao-Lian Zhang

panqincn@whu.edu.cn (Q.P.)
zhangxiaolian@whu.edu.cn (X.-L.Z.)

HIGHLIGHTS

Mtb mannose-capped lipoarabinomannan (ManLAM) induces IL-10 production in B cells

ManLAM-induced B10 cells enrich in CD5^{+} B1a B cells

ManLAM binding with TLR2 triggers MyD88 signaling pathways of B cells

ManLAM-induced B10 cells hinder CD4^{+}Th1 immunity during Mtb infection in mice

Yuan et al., iScience *11*, 13–30
January 25, 2019
https://doi.org/10.1016/j.isci.2018.11.039

iScience

CellPress

Article

Mycobacterium tuberculosis Mannose-Capped Lipoarabinomannan Induces IL-10-Producing B Cells and Hinders CD4^{+}Th1 Immunity

Chunhui Yuan,[1,2,3] Zi-Lu Qu,[1,3] Xiao-Lei Tang,[1] Qi Liu,[1] Wei Luo,[1] Chun Huang,[1] Qin Pan,[1,*] and Xiao-Lian Zhang[1,4,*]

SUMMARY

The importance of Th1/interferon (IFN)-γ-mediated responses in mycobacterial infection has been well established. However, little is known about B cell-mediated immunity during *Mycobacterium tuberculosis* (Mtb) infection. Interleukin (IL)-10-producing B cells (B10 cells), a subset of B regulatory cells (Bregs), are implicated in modulating the immune response. Herein, we found that B10 cells were significantly increased in patients with tuberculosis. Furthermore, mannose-capped lipoarabinomannan (ManLAM), a major surface lipoglycan component from Mtb, induced a significant increase in B10 cells, which enriched in CD5^{+} B1a B cells. ManLAM induced IL-10 production mainly by activating MyD88/PI3K/AKT/Ap-1 and K63-linked ubiquitination of NF-κB essential modulator/nuclear factor kappa-light-chain-enhancer of activated B cells signaling pathways in B cells via Toll-like receptor 2. IL-10 production by ManLAM-treated B cells further inhibited CD4^{+} Th1 polarization, leading to increased susceptibility to mycobacterial infection compared with ManLAM-treated IL-10$^{-/-}$ B group. Thus, we report a new immunoregulation mechanism in which Mtb ManLAM-induced B10 cells negatively regulate host anti-TB cellular immunity.

INTRODUCTION

Tuberculosis (TB) is the leading cause of death due to infectious diseases worldwide. In 2016, the World Health Organization reported approximately 10.4 million new TB cases worldwide (World Health Organization, 2017). The emergence of multidrug-resistant TB and co-infection with the human immunodeficiency virus (HIV) make TB control even more urgent. An attenuated strain vaccine of *Mycobacterium bovis*, termed bacillus Calmette–Guérin (BCG), the only available used TB vaccine, still has limited protective efficacy against TB. Therefore, it is important to understand the bacterial immunoregulation mechanism and host immune defense mechanisms against mycobacteria.

Characterization of the immune response to *Mycobacterium tuberculosis* (Mtb) has largely focused on Th1 cell-mediated immunity, whereas B cells are often overlooked in anti-Mtb immunity. Recently, emerging evidence suggests that B cells may orchestrate the immune response against Mtb by interacting with other immune cells such as T cells (Achkar et al., 2015; Hoff et al., 2015; Kozakiewicz et al., 2013; Maglione et al., 2007). Regulatory B cells (Bregs), which produce interleukin (IL)-10 or transforming growth factor β, participate in the immunomodulation of immune responses. A subset of Bregs, IL-10-producing B cells (B10 cells), has been shown to prevent excessive inflammatory responses in autoimmune diseases (Mauri et al., 2012; Yang et al., 2013). B10 cells also appear to negatively regulate cellular immune responses in infectious diseases caused by intracellular pathogens, including hepatitis B virus (Das et al., 2012), HIV-1 (Liu et al., 2014a, 2014b), and *Listeria* (Horikawa et al., 2013). However, the roles of B10 cell in the immune response to Mtb remain elusive.

Mannose-capped lipoarabinomannan (ManLAM) is a major cell wall lipoglycan and an important immunomodulatory component of mycobacteria (Mishra et al., 2011). Bacterial ManLAM can also be secreted and recognized by macrophages and dendritic cells (DCs) via pattern recognition receptors, including mannose receptor (MR), Toll-like receptor 2 (TLR2), DC-specific intercellular adhesion molecule-3-grabbing non-integrin (DC-SIGN), CD1d, sphingosine-1-phosphate receptor 1 (S1P1), Dectin-2, and CD44, and triggers several cell signaling pathways (Pan et al., 2014; Osanya et al., 2011; Geijtenbeek et al., 2003; Sun et al., 2016; Richmond et al., 2012; Yonekawa et al., 2014; Zajonc et al., 2006). ManLAM inhibits

[1]State Key Laboratory of Virology and Medical Research Institute, Hubei Province Key Laboratory of Allergy and Immunology and Department of Immunology, Wuhan University School of Basic Medical Sciences, Wuchang, Wuhan 430071, China

[2]Department of Laboratory Medicine, Wuhan Children's Hospital, Huazhong University of Science and Technology, Jiangan, Wuhan 430015, China

[3]These authors contributed equally

[4]Lead Contact

*Correspondence: panqincn@whu.edu.cn (Q.P.), zhangxiaolian@whu.edu.cn (X.-L.Z.)

https://doi.org/10.1016/j.isci.2018.11.039

phagosome maturation in macrophages, DC maturation, and $CD4^+$ T cell activation (Osanya et al., 2011; Fratti et al., 2003; Mahon et al., 2012). Anti-ManLAM antibody treatment and anti-ManLAM aptamer treatment decrease bacterial loads and dissemination, prolong survival, and lead to better disease outcomes in an animal model of TB (Pan et al., 2014; Hamasur et al., 2004).

We were interested in determining the interaction between ManLAM and B cells. In the present study, we first reported that ManLAM induced IL-10 production by B cells (B10 cells) both *in vitro* and *in vivo* predominantly through TLR2. Molecular mechanism analysis revealed that the binding of ManLAM to TLR2 activated MyD88 and its downstream AP1 and nuclear factor kappa-light-chain-enhancer of activated B cells (NF-κB) signaling to promote IL-10 production by B cells. ManLAM-induced B10 cells hindered Th1 response compared with ManLAM-IL-$10^{-/-}$ B cells, facilitating mycobacterium survival. We report a new immunoregulation mechanism in which Mtb ManLAM-induced B10 cells negatively regulate host anti-TB cellular immunity. Our findings will help to understand the interaction between B cells and Mtb ManLAM and highlight the ManLAM-mediated B10 cells' immunomodulatory functions.

RESULTS

Peripheral B10 Cells Are Elevated in Patients with TB

To assess the roles of human B10 cells in TB disease, we determined the serum concentration of IL-10 and the frequency of B10 cells in patients with active pulmonary TB. As shown in Figure 1A, the serum IL-10 concentrations in patients with active TB (ATB) were much higher than those in healthy donors (161.2 ± 21.34 pg/mL versus 40.9 ± 6.6 pg/mL). Consistent with the elevated serum IL-10 level, the percentages of IL-10^+CD19^+ B cells in peripheral blood mononuclear cells from patients with TB were significantly increased compared with those from healthy donors (4.0% ± 0.3% versus 1.0% ± 0.7%; Figures 1B and 1C). These results indicated that increased levels of IL-10 and B10 cells in patients with TB might be associated with TB disease.

Because ManLAM is a virulent factor of Mtb, we determined the serum ManLAM concentrations in patients with ATB. We observed significantly higher serum levels of ManLAM in 30 patients with ATB (156.1 ng/mL, 95% confidence interval [CI] = 95.5–216.6) compared with those of 30 healthy donors (8.8 ng/mL, 95% CI = 6.8–10.8, Figure 1D). These results indicated that Mtb ManLAM might be related to the increase in serum IL-10 level in patients with ATB.

ManLAM Induces Murine B10 Cells *In Vitro* and *In Vivo*

To elucidate the roles of B10 cells in the immune response to Mtb, we first determined whether Mtb and ManLAM induced IL-10 production by murine B cells *in vitro*. Mtb H37Rv/BCG ManLAM was purified from the bacteria (Figures S1A and S1B). It has been reported that *Mycobacteria* do not have endotoxin (Jackson, 2014) (known as lipopolysaccharide [LPS]). The ManLAM used in our experiments was not contaminated by endotoxin because endotoxin scavenger polymyxin B-treated-ManLAM did not significantly alter IL-10 production and the cytotoxicity against B cells compared with ManLAM treatment (Figures S1C and S1D). According to the previous report (Kishimoto, 1985), we used IL-2 to promote B cell proliferation in our experiments. Both IL-2 and IL-4 had been used to promote B cell proliferation (Kishimoto, 1985; Karray et al., 1988; Wagner et al., 1998). However, IL-4 had the potential ability to negatively control B cell differentiation (Bod et al., 2018) and could inhibit IL-10 production by B cells upon stimulation with IL-5/mCD40L-expressing fibroblast in a STAT6-dependent manner (Taitano et al., 2018). Therefore, we used IL-2 to promote B cell proliferation in the current study. As shown in Figure S1C, the addition of IL-2 alone did not significantly affect the IL-10 production by B cells compared with the medium control group.

Flow cytometry (FCM) analysis showed that iH37Rv, iBCG (heat-inactivated Mtb H37Rv and BCG, in which heat-inactivated bacterial proteins were denatured [Ferrier, 2017], but bacterial glycolipids maintained activities [Worakitkanchanakul et al., 2008]), and ManLAM purified from both Mtb H37Rv and BCG significantly induced $CD19^+$ B cells into B10 cells compared with the IL-2 control groups (Figures 2A, 2B, and S1E). As shown in Figures 2B and S1E, iBCG induced more B10 cells than iBCGΔ2196 (a ManLAM mutant strain of BCG that lacks the mannose cap of ManLAM) (Sun et al., 2016). These results demonstrated that Mtb ManLAM induced B10 cells *in vitro*.

The IL-10 levels produced by the ManLAM-treated B cells were further measured. As shown in Figure 2C, both ManLAM and iH37Rv significantly induced IL-10 levels approximately 6- to 7-fold higher than that of

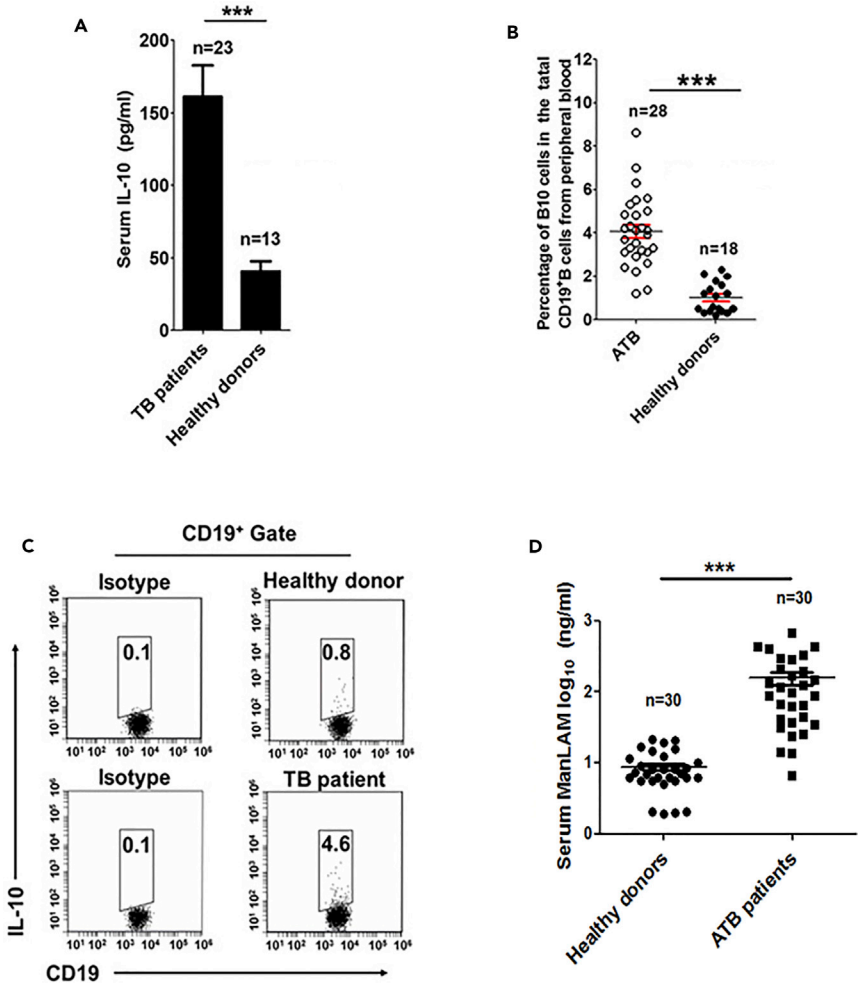

Figure 1. Elevated Levels of B10 Cells in Peripheral Blood of Patients with TB

(A) Elevated serum IL-10 level in patients with ATB. IL-10 was detected by ELISA. Data are represented as mean ± SD. Two-tailed, unpaired t test; ***$p < 0.001$.

(B and C) (B) Human B10 cells were determined by flow cytometry analysis. (C) Representative dot plots. Data are represented as mean ± SD. ***$p < 0.001$.

(D) Serum ManLAM levels in patients with ATB and healthy donors. MR was coated on the microplates, and then the serum samples were added on the microplates. After washing, the biotin-labeled single-stranded DNA aptamer T9 (400 nM) was added to detect serum ManLAM and the horseradish peroxidase-streptavidin conjugate was used for color development. The absorbance at 450 nm was determined. Data are represented as mean ± SD. ***$p < 0.001$.

the IL-2 control group and approximately 1- to 2-fold higher than that of the LPS-treated group. Both B10 cell numbers and IL-10 concentrations reached peak level approximately at 12 hr upon stimulation with ManLAM, and then slowly decreased, but were still higher than those in the control group (Figures 2D and S1F). The highest IL-10 and B10 cell levels were induced upon stimulation with 10 ng/mL ManLAM (Figures 2E and S1G). As shown in Figure 2F, the frequencies of B10 cells in $CD1d^{hi}CD5^{+}$ B and $CD1d^{lo}CD5^{+}$ B subsets were 17.1% and 12.4%, respectively, in ManLAM treatment group, which were much higher than the B10 frequencies in $CD1d^{hi/lo}CD5^{-}$ B cells. Therefore, we identified ManLAM-induced B10 cells enriched in $CD5^{+}$ B1a B cells ($CD1d^{hi/lo}CD5^{+}$ B cells). $CD1d^{hi}CD5^{+}$ B cell population contains several B cell subsets, including marginal zone B cells and B1 B cells (Yanaba et al., 2008), which can be rapidly recruited into the early adaptive immune responses in a T cell-independent manner. The function of $CD1d^{lo}CD5^{+}$ B cells are unknown, but Ding et al. reported that some $CD1d^{lo}CD5^{+}$ B cells can secrete IL-10 as well (Ding et al., 2011). In the LPS group, LPS-induced B10 cells enriched in $CD1d^{hi}CD5^{+}$ B cells (22.9%), which was consistent with the previous report (Matsushita and Tedder. 2011).

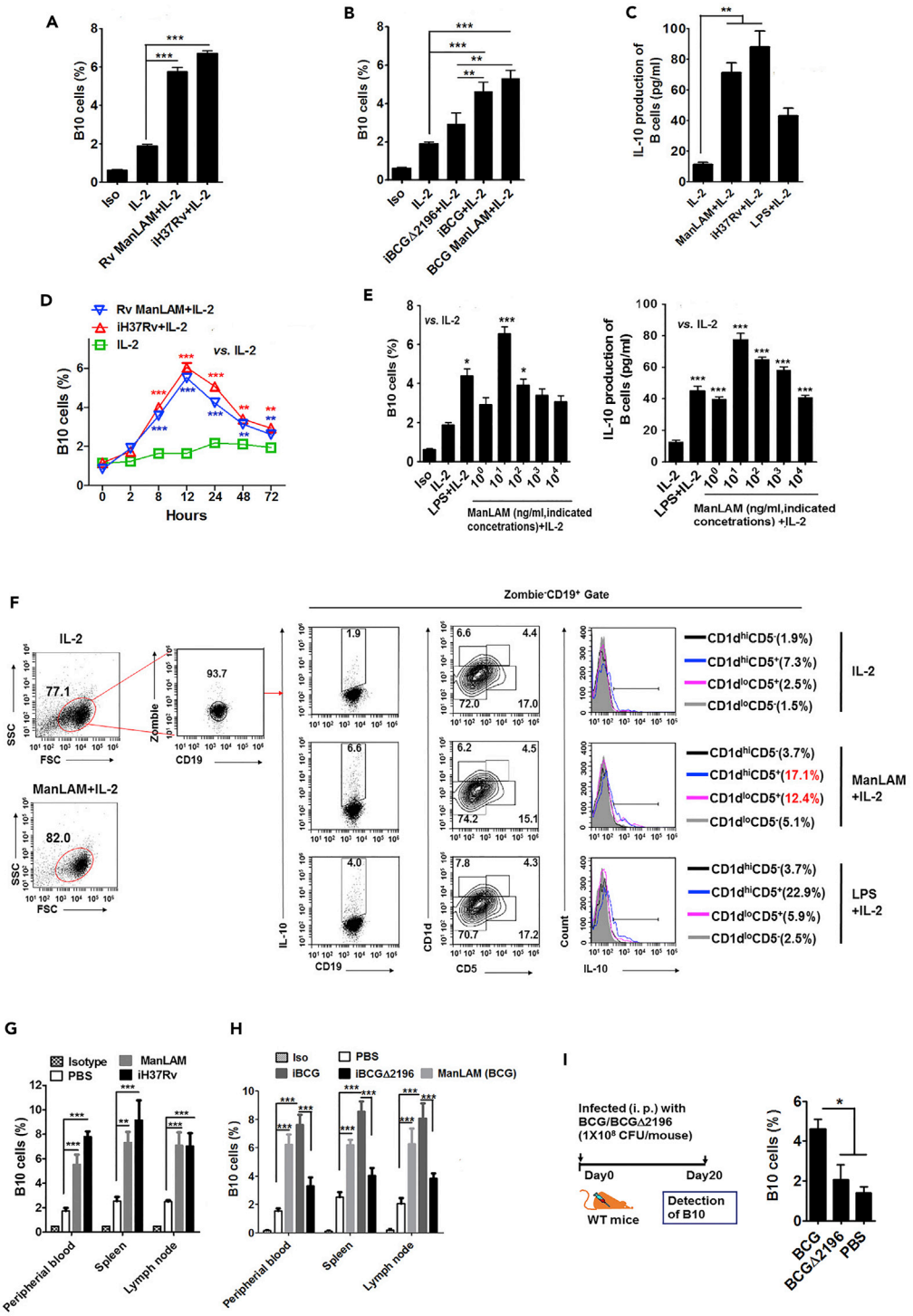

Figure 2. BCG/iH37Rv/ManLAM Induces B10 Cells, whereas BCGΔ2196 Induces Less B10 Cells *In Vitro* and *In Vivo*

(A and B) B10 cells were detected by flow cytometry (FCM). B cells were stimulated with iH37Rv (MOI, 1:2) or Rv ManLAM (10 ng/mL), iBCG (MOI, 1:2), iBCGΔ2196 (MOI, 1:2), or BCG ManLAM (10 ng/mL) for 12 hr. Data are represented as mean ± SD. ***$p < 0.001$, **$p < 0.01$.

(C) IL-10 production in culture supernatant was detected by ELISA. B cells were stimulated with Rv ManLAM, LPS (10 μg/mL) or iH37Rv for 12 hr. Data are represented as mean ± SD. **$p < 0.01$.

Figure 2. *Continued*

(D) Time course of IL-10 production in ManLAM-treated B cells. B10 cells were detected by FCM. Data are represented as mean ± SD. ***$p < 0.001$, **$p < 0.01$.

(E) IL-10 production by B cells stimulated with various concentrations of ManLAM for 12 hr. Data are represented as mean ± SD. ***$p < 0.001$, *$p < 0.05$.

(F) B10 cells enriched in $CD5^+$ B1a B cells ($CD1d^{hi/lo}CD5^+$ B cells) upon Rv ManLAM stimulation for 12 hr.

(G and H) B cells produced IL-10 upon stimulation with iH37Rv/iBCG/iBCGΔ2196/ManLAM *in vivo*. WT (C57BL/6J) mice were injected (intraperitoneally [i.p.]) with iH37Rv/iBCG/iBCGΔ2196 (10^8 CFU/100 μL/mouse) or ManLAM (100 ng/100 μL/mouse), and each group had six mice; B10 cells were analyzed by FCM. Data are represented as mean ± SD. ***$p < 0.001$, **$p < 0.01$.

(I) WT mice were infected (i.p.) with BCG/BCGΔ2196 (6 mice/group). Left panel: schematic diagram. Right panel: splenocytes were collected at day 20 post-infection. B10 cells were determined by FCM. Data are represented as mean ± SD. *$p < 0.05$.

(A–E) B cells were cultured in medium containing IL-2.

See also Figure S1.

ManLAM-induced B10 cells were then detected *in vivo*. Mice were intraperitoneally injected with purified ManLAM (from Mtb H37Rv/BCG), iH37Rv/iBCG/iBCGΔ2196, at days 1 and 7. After the second injection, we observed increased B10 cells in peripheral blood, spleens, and lymph nodes from the mice subjected to the ManLAM, iH37Rv, and iBCG treatment, respectively (Figures 2G, 2H, S1H, and S1I), whereas iBCGΔ2196 induced less B10 cells than BCG (Figure 2H). The B10 cell percentage was also significantly higher in the live BCG infection group compared with the PBS and live BCGΔ2196 infection groups (Figures 2I and S1J). These results indicated that B10 cells were induced by Mtb and ManLAM both *in vitro* and *in vivo* (Figures 2A–2I and S1C–S1J).

ManLAM Induces IL-10 Production by B Cells Mainly via TLR2

It has been reported that ManLAM can be recognized by TLR2 and MR (Pan et al., 2014; Osanya et al., 2011). Both TLR2 and MR signals are involved in IL-10 production by macrophages and monocytes during Mtb infection (Sun et al., 2016; Wang et al., 2012). Therefore, we investigated whether TLR2 and MR were involved in ManLAM-induced IL-10 production in B cells.

In the pull-down and immunoblotting assay, both TLR2 and MR were identified as ManLAM-associated proteins from wild-type (WT) B cells (Figure 3A). ManLAM lost the ability to bind to TLR2 in $TLR2^{-/-}$ B cells and showed decreased binding to MR in MR-short hairpin RNA (shRNA)-treated B cells (Figures 3A, S2A, and S2B), which further supported the binding of ManLAM to both TLR2 and MR. In the competition assay, the binding of TLR2 to ManLAM was not inhibited by a soluble MR competitor, and soluble TLR2 competitor did not inhibit MR binding to ManLAM (Figure S2C). This finding indicated that the binding sites of ManLAM for MR and TLR2 were different.

Next, we assessed whether the binding of ManLAM to MR and TLR2 participated in IL-10 production by B cells. As shown in Figure 3B, MR knockdown in both WT and $TLR2^{-/-}$ B cells had little effect on IL-10 production compared with the scramble group after ManLAM stimulation. IL-10 production was markedly reduced in $TLR2^{-/-}$ B cells, but not in $TLR4^{-/-}$ B cells and WT B cells after ManLAM treatment (Figure 3C). These findings suggest that ManLAM-MR binding has only a minor effect on IL-10 production by B cells but ManLAM-TLR2 binding is involved in IL-10 production in ManLAM-treated B cells.

We found that ManLAM induced IL-10 production by $TLR2^{-/-}$ B cells was significantly decreased by approximately 60%–80% compared with the WT B cell control or $TLR4^{-/-}$ B cells (Figures 3C–3E). Blocking ManLAM binding to TLR2 by anti-TLR2 antibody significantly decreased IL-10 production in WT B cells (Figure S2D). Moreover, the $TLR2^{-/-}$ B cells were actually capable of producing IL-10 at similar levels to WT B cells when the cells were stimulated with LPS and anti-IgM+ CD40 (Figure S2E). There was no significant difference in IL-10 production between $TLR4^{-/-}$ B and WT B cells upon ManLAM stimulation (Figures 3C–3E). These results strongly confirmed that ManLAM induced IL-10 production by B cells predominantly via TLR2.

To assess the effects of ManLAM as well as other TLR ligands on IL-10 production by B cells, ManLAM, TLR1/2 agonist Pam3CSK4, TLR6/2 agonist FSL-1 (synthetic diacylated lipoprotein), TLR4 agonist LPS, and TLR5 agonist FLA-ST (flagellin from *Salmonella typhimurium*) were used. As shown in Figure S2F, the B10 levels were increased in the ManLAM, TLR1/2 agonist, TLR6/2 agonist, and TLR4 agonist groups, whereas the B10 cell level did not change after treatment with TLR5 agonist. ManLAM induced IL-10

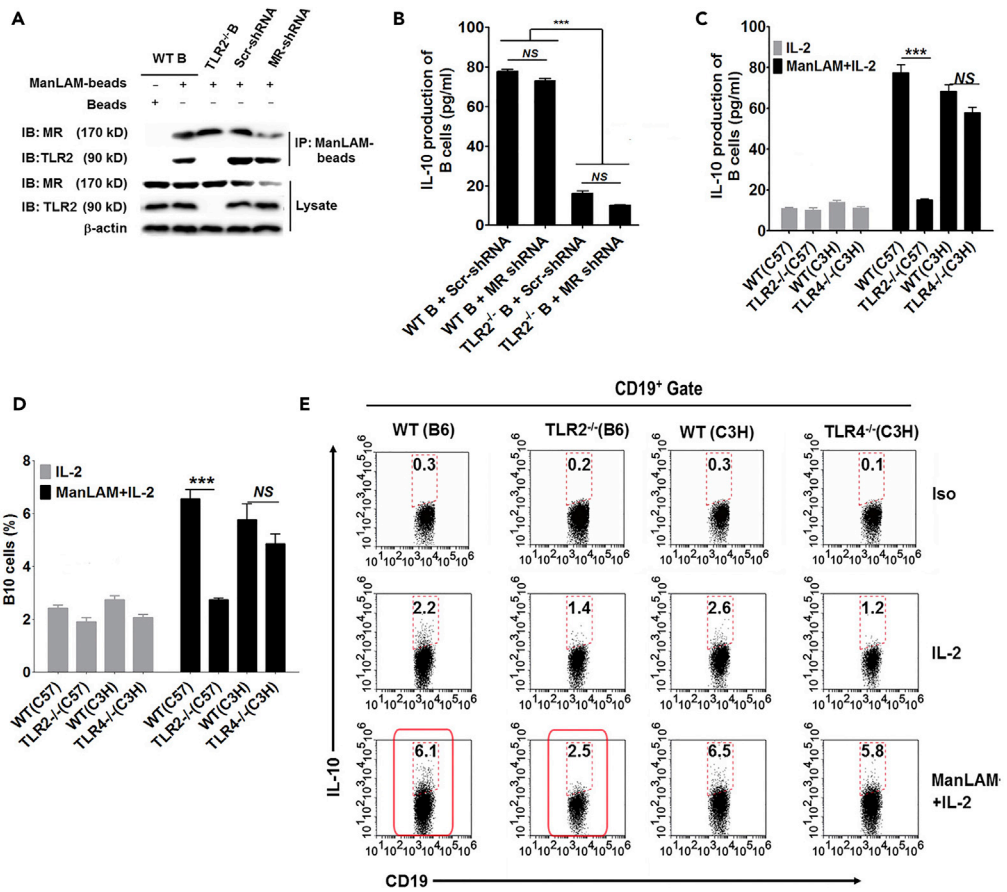

Figure 3. ManLAM Induces IL-10 Production by B Cells Mainly via TLR2

(A) Binding of ManLAM to TLR2 and MR proteins was detected by immunoblotting. Cell lysates from WT B cells, TLR2$^{-/-}$ B cells, and MR shRNA-transfected B cells were incubated with Rv ManLAM-coupled magnetic beads.

(B) IL-10 production by ManLAM-treated B cells was not mainly via MR. WT/TLR2$^{-/-}$ B cells were transfected with MR shRNA for 48 hr and stimulated with ManLAM (10 ng/mL) for 12 hr. IL-10 production in cell supernatant was detected by ELISA. Data are represented as mean ± SD. ***$p < 0.001$; NS, not significant.

(C–E) IL-10 production by ManLAM-treated B cells was dominantly via TLR2. Splenic B cells were stimulated with ManLAM for 12 hr. (C) IL-10 in culture supernatant was detected by ELISA. (D) B10 cells were analyzed by flow cytometry. (E) Representative dot plots. Data are represented as mean ± SD. ***$p < 0.001$; NS, not significant.

(B–E) B cells were cultured in medium containing IL-2.

See also Figures S2 and S3.

through TLR2, but this was not specific for ManLAM. The ligands for TLR2 could also induce IL-10 production by B cells.

TLR2 is working in heterodimers with TLR1 or TLR6. To further identify the roles of TLR2 heterodimers, we used TLR1 and TLR6 antagonists to assess the mechanism of IL-10 production by ManLAM-treated B cells. As shown in Figure S2G, either TLR1/2 or TLR2/6 heterodimers were involved in IL-10 production of ManLAM-treated B cells because ManLAM induced much lower levels of IL-10 in the presence of TLR1 or TLR6 antagonists. We used TLR1-shRNA and TLR6-shRNA to silence TLR1 and TLR6 expression on B cells (Figures S2H and S2I). Consistent with the above-mentioned results, the IL-10 production by TLR1 (or TLR6)-silenced B cells was greatly reduced upon stimulation with ManLAM (Figure S2J). These data suggest that ManLAM induces IL-10 production by B cells via TLR1/2 or TLR2/6 heterodimers.

It has been reported that ManLAM can be recognized by other receptors, including DC-SIGN, CD1d, $S1P_1$, Dectin-2, and CD44, and triggers several cell signaling pathways (Geijtenbeek et al., 2003; Sun et al., 2016; Richmond et al., 2012; Yonekawa et al., 2014; Zajonc et al., 2006). However, DC-SIGN and Dectin-2 are

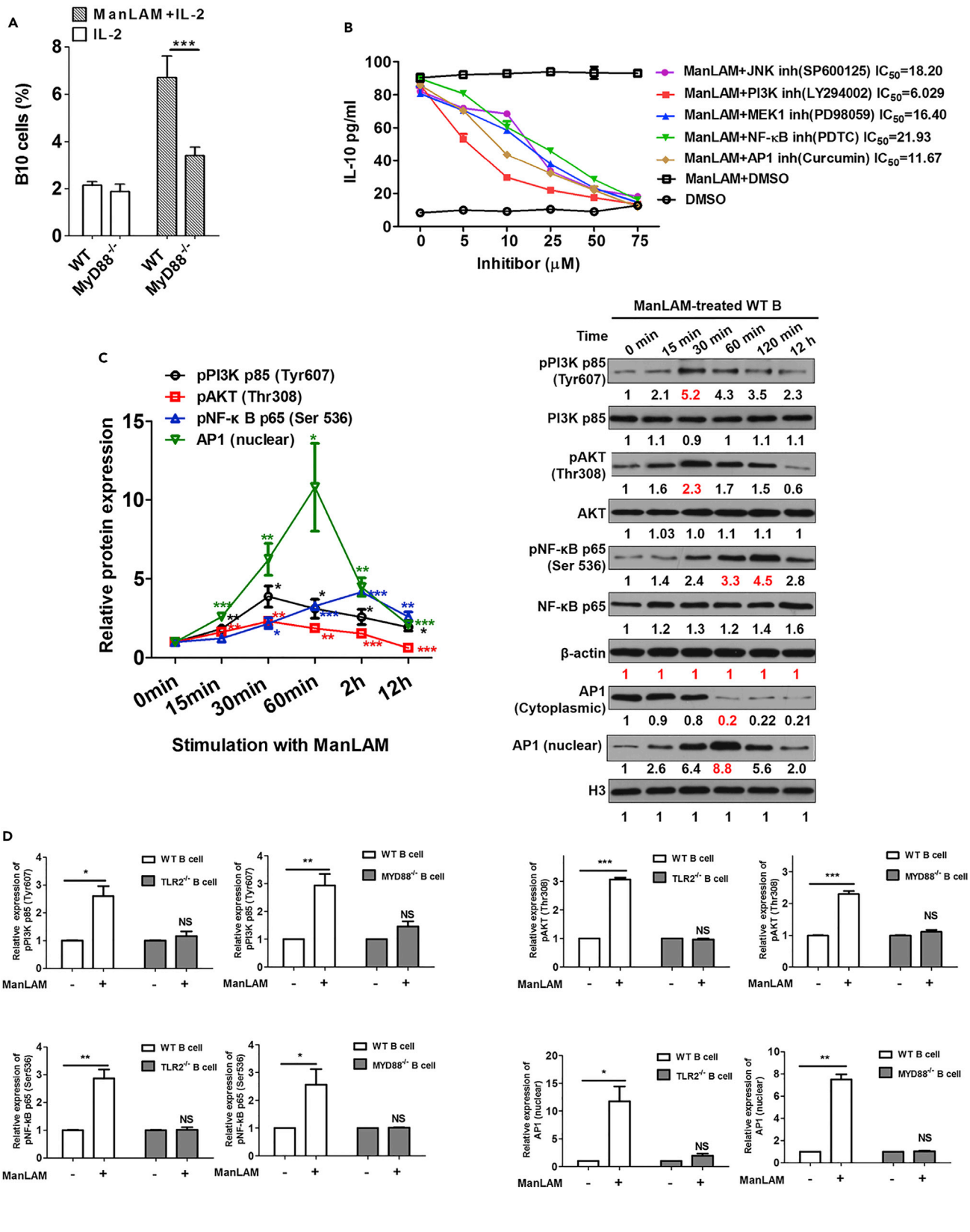
A
ManLAM+IL-2
IL-2
B10 cells (%)
***
WT
MyD88-/-
WT
MyD88-/-
B
IL-10 pg/ml
Inhitibor (μM)
ManLAM+JNK inh(SP600125) IC50=18.20
ManLAM+PI3K inh(LY294002) IC50=6.029
ManLAM+MEK1 inh(PD98059) IC50=16.40
ManLAM+NF-κB inh(PDTC) IC50=21.93
ManLAM+AP1 inh(Curcumin) IC50=11.67
ManLAM+DMSO
DMSO
C
pPI3K p85 (Tyr607)
pAKT (Thr308)
pNF-κ B p65 (Ser 536)
AP1 (nuclear)
Relative protein expression
0min
15min
30min
60min
2h
12h
Stimulation with ManLAM
ManLAM-treated WT B
Time
0 min
15 min
30 min
60 min
120 min
12 h
pPI3K p85 (Tyr607)
1 2.1 5.2 4.3 3.5 2.3
PI3K p85
1 1.1 0.9 1 1.1 1.1
pAKT (Thr308)
1 1.6 2.3 1.7 1.5 0.6
AKT
1 1.03 1.0 1.1 1.1 1
pNF-κB p65 (Ser 536)
1 1.4 2.4 3.3 4.5 2.8
NF-κB p65
1 1.2 1.3 1.2 1.4 1.6
β-actin
1 1 1 1 1 1
AP1 (Cytoplasmic)
1 0.9 0.8 0.2 0.22 0.21
AP1 (nuclear)
1 2.6 6.4 8.8 5.6 2.0
H3
1 1 1 1 1 1
D
Relative expression of pPI3K p85 (Tyr607)
WT B cell
TLR2-/- B cell
MYD88-/- B cell
NS
ManLAM
Relative expression of pAKT (Thr308)
Relative expression of pNF-κB p65 (Ser536)
Relative expression of AP1 (nuclear)

Figure 4. ManLAM-TLR2 Binding Stimulates IL-10 Production in B Cells by Activating MyD88/PI3K/AKT/Ap-1 and NF-κB Signaling Pathways

(A) B10 cells were analyzed by flow cytometry. WT and MyD88$^{-/-}$ B cells were stimulated with Rv ManLAM (10 ng/mL) for 12 hr. Data are represented as mean ± SD. ***p < 0.001.

(B) IL-10 production in ManLAM-treated B cells was inhibited by inhibitors of JNK, PI3K, MEK1, AP-1, and NF-κB. B cells were pretreated with the inhibitors for 1 hr. The cells were stimulated with ManLAM. IL-10 production in the supernatant was determined by ELISA.

(C) PI3K, AKT, AP1, and NF-κB activation in WT B cells upon ManLAM stimulation were analyzed at multiple time points by immunoblotting. Left panel: pooled data. Right panel: representative blots. Data are represented as mean ± SD versus 0 min at indicated time. ***p < 0.001, **p < 0.01,*p < 0.05.

(D) PI3K, AKT, NF-κB, and AP1 activation were determined in WT B cells and TLR2$^{-/-}$ B cells (or MyD88$^{-/-}$ B cells) upon stimulation with ManLAM for 1 hr by immunoblotting. Data are represented as mean ± SD. ***p < 0.001, **p < 0.01, *p < 0.05; NS, not significant.

(A–D) B cells were cultured in medium containing IL-2.

See also Figure S4.

undetectable in B cells (Ariizumi et al., 2000; Soilleux et al., 2002). The binding of ManLAM to CD44 is involved in the downregulation of IL-10 production (Sun et al., 2016). Therefore, we investigated whether CD1d and S1P$_1$ were involved in ManLAM-induced IL-10 production by B cells. CD1d monoclonal antibody (mAb) blocked ManLAM-CD1d binding in a dose-dependent manner (Figures S3A). However, the addition of CD1d mAb did not reduce IL-10 production by ManLAM-treated B cells (Figures S3B, S3C, and S3E). The results indicated that ManLAM-CD1d binding was not involved in triggering IL-10 production by B cells. The S1P$_1$ inhibitor W146 slightly reduced ManLAM-induced IL-10 production by B cells (approximately 20%, Figures S3D and S3E). Taken together, our findings demonstrated that ManLAM induced IL-10 production of B cells predominantly through TLR2.

ManLAM Induces IL-10 Production by B Cells via TLR2/MyD88/Ap-1 and K63-Linked Ubiquitination of NEMO/NF-κB Signaling Pathways

The signaling pathways in B cells that lead to IL-10 production have thus far remained elusive (Mauri and Bosma, 2012). We chose several key adapter proteins and transcription factors downstream of TLR2 to explore the signaling pathway that might contribute to IL-10 production in ManLAM-treated B cells (Du et al., 2016; Gaddis et al., 2013; Hu et al., 2006; Liu et al., 2014a, 2014b; Saraiva and O'Garra, 2010).

As shown in Figures 4A and S4A, IL-10 production was significantly reduced by approximately 60%–80% in MyD88$^{-/-}$ B cells, demonstrating that MyD88 was involved in IL-10 production in ManLAM-treated B cells. Specific inhibitors were applied to inhibit the activation of JNK (c-Jun N-terminal kinase), PI3K (phosphoinositide-3 kinase), MEK1 (mitogen-activated extracellular signal-regulated kinase 1), NF-κB, and AP1 (activator protein 1) in ManLAM-treated B cells. As shown in Figures 4B, S4B, and S4C, ManLAM-induced IL-10 production was significantly inhibited by inhibitors of the upstream signal transducers JNK, PI3K, and MEK1, as well as AP-1 and NF-κB. The two most potent inhibitors were PI3K (half maximal inhibitory concentration [IC$_{50}$] = 6.029 μM) inhibitor and AP1 inhibitor (IC$_{50}$ = 11.67 μM, Figures 4B, S4B, and S4C).

Immunoblotting analysis revealed that PI3K and its downstream target AKT were highly phosphorylated at 30 min after ManLAM stimulation (Figure 4C). We found that cytoplasmic AP1, a downstream effector of PI3K/AKT, was decreased and nuclear AP1 was greatly increased 60 min after ManLAM stimulation (Figure 4C). The peak of NF-κB activation occurred between 60 and 120 min after ManLAM stimulation (Figure 4C). Both TLR2$^{-/-}$ B cells and MyD88$^{-/-}$ B cells showed a blunted increase in PI3K and AKT phosphorylation, nuclear AP1, and NF-κB activation upon ManLAM stimulation (Figures 4D and S4D).

As shown in Figures S4E and S4F, we did not observe ManLAM signaling and IL-10 production when (1) TLR2$^{-/-}$ B cells were treated with ManLAM/Pam3CSK4 and (2) WT B cells were stimulated with ManLAM/Pam3CSK4 in the presence of MyD88 inhibitor (ST2825). Therefore ManLAM signaling occurred predominantly through the TLR2-MyD88 pathway, and no compensatory pathway was detected. As shown in Figure S4G, knockdown of MR in TLR2$^{-/-}$ B cells had fairly limited effects on ManLAM signaling, further confirming that MR has only a minor effect on B10 cells. Taken together, these results suggested that ManLAM induced IL-10 production by B cells mainly via the TLR2/MyD88/PI3K/AKT/AP-1 and NF-κB signaling pathways.

It has been reported that the Lys63 (K63)-linked ubiquitination of NF-κB essential modulator ([NEMO] also known as IKK-γ) is involved in the IKK complex recruitment for NF-κB activation, whereas Lys48 (K48)-linked ubiquitination is associated with proteasomal degradation and inhibits NF-κB activation (Lopez-Castejon and Edelmann, 2016). As shown in Figure 5A, K63 polyubiquitylation, but not K48 polyubiquitylation, of NEMO was observed in ManLAM-treated B cells.

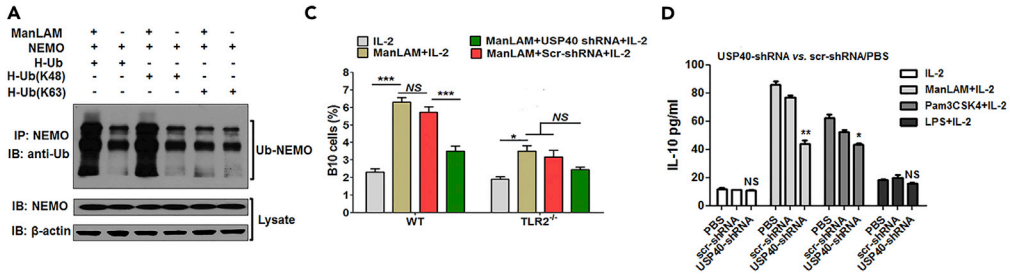

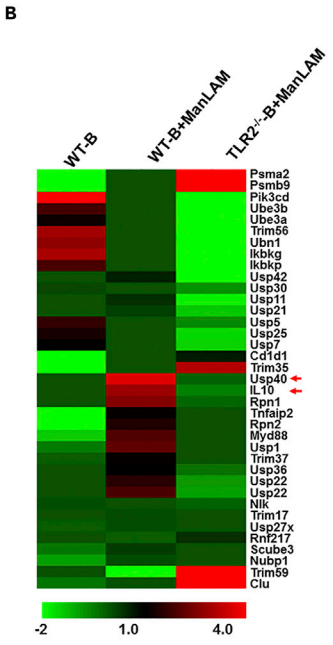

Relative expression of ubiquitination, MyD88/AP-1 and NF-κB signal-related mRNA

Symbol	WT-B (FPKM)	WT-B+ ManLAM (FPKM)	TLR2$^{-/-}$-B+ ManLAM (FPKM)	Log_2Fold Change (WT-B+ManLAM *vs.* TLR2$^{-/-}$-B+ManLAM)	Regulation
Il10	2.45	5.31	1.92	2.559	up
Usp40	5.07	8.73	4.89	1.365	up
Nlk	8.64	8.58	8.39	1.010	down
Ikbkap	10.49	10.89	8.64	1.107	up
Ikbkg	13.64	13.52	12.8	1.021	up
Tnfaip2	2.5	6.52	5.39	1.112	up
Scube3	1.29	1.98	1.73	1.246	up
Ube3b	31.22	29.37	24.66	1.054	up
Ube3a	19.07	17.86	11.95	1.161	up
Trim56	17.96	15	8.35	1.276	up
Trim37	4.62	5.86	4.76	1.133	up
Rpn1	29.03	31.61	28.8	1.027	up
Rpn2	51.59	55.18	53.76	1.006	up
Cd1d1	17.32	22.56	23.21	0.990	down
Myd88	24.46	27.87	25.89	1.022	up
Pik3cd	113.52	100.57	86.11	1.034	up
Ubn1	29.28	26.56	19.85	1.097	up
Psma2	77.42	87.99	105.62	0.960	down
Psmb9	80.41	83.82	117.45	0.929	down
Trim17	0.36	0.48	0.38	0.758	up
Usp11	22.23	20.88	19.31	1.026	up
Trim35	34.91	39.18	42.31	0.979	down
Usp42	10.19	10.43	8.81	1.077	up
Trim59	39.55	36.14	45.67	0.938	down
Usp7	59.01	55.97	52.53	1.016	up
Usp25	34.45	32.56	29.29	1.031	up
Usp22	21.36	22.87	20.53	1.035	up
Usp1	27.73	30.39	28.21	1.022	up
Usp36	16.51	17.5	16.15	1.028	up
Usp5	32.8	33.4	29.54	1.036	up
Usp27x	0.46	0.61	0.56	0.852	up
Usp30	14.36	12.72	12.06	1.021	up
Usp21	23.39	22.42	20.91	1.022	up
Trim28	75.9	77.83	75	1.008	up
Rnf217	0.23	0.09	0.65	5.589	down
Nubpl	3.24	4.2	4.13	1.011	up
Clu	0.76	1.17	8.06	0.075	down

Figure 5. K63-Linked Ubiquitination of NEMO and USP40 Are Involved in TLR2-Dependent IL-10 Production in ManLAM-Treated B Cells

(A) ManLAM induces K63-linked ubiquitination of NEMO in B cells. B cells were transfected with the plasmids encoding NEMO, wild-type (WT) ubiquitin (H-Ub), ubiquitin mutant H-Ub (K48), and H-Ub (K63). After stimulation with Rv ManLAM, the supernatant from cell lysates was subjected to immunoprecipitation and immunoblotting (upper panel). The expression levels of NEMO were examined by immunoblotting (lower panel).

(B) The mRNA expression levels of NF-κB signal and ubiquitination-related proteins in ManLAM-treated CD1d^{hi}CD5^{+} B cells were determined by transcriptome analysis. Left panel: differentially expressed mRNAs were presented as a heatmap. The threshold established for upregulated and downregulated genes was a log2 fold change ≥ 1.0. Red, upregulation; green, downregulation. Right panel: mRNA expression levels. FPKM (fragments per kilobase million) value indicated the relative expression of genes.

(C and D) ManLAM induces B10 cells via TLR2 and USP40. B cells were transfected with USP40-shRNA and stimulated with ManLAM. (C) B10 cells and (D) IL-10 production were detected by flow cytometry and ELISA. Data are represented as mean ± SD. ***$p < 0.001$, **$p < 0.01$, *$p < 0.05$; NS, not significant.

(A–D), B cells were cultured in medium containing IL-2.

See also Figure S5.

Because the highest frequency of ManLAM-induced B10 cells was found in CD1d^{hi}CD5^{+} B subset, we sorted CD1d^{hi}CD5^{+} B cells from the spleens of both WT and TLR2$^{-/-}$ mice and analyzed global gene expression changes by RNA sequencing after ManLAM treatment (Figures 5B, S5A, and S5B). The gene ontology analysis (Figure S5A) identified differentially expressed genes involved including 24 biological processes, 15 cellular components, and 10 molecular functions (false discovery rate, FDR ≤ 0.01) in the WT group compared with the TLR2$^{-/-}$ group. Also, biological processes include the response to stimulus and immune system process (Figure S5A). Chemokine signaling pathway and NF-κB signaling pathway

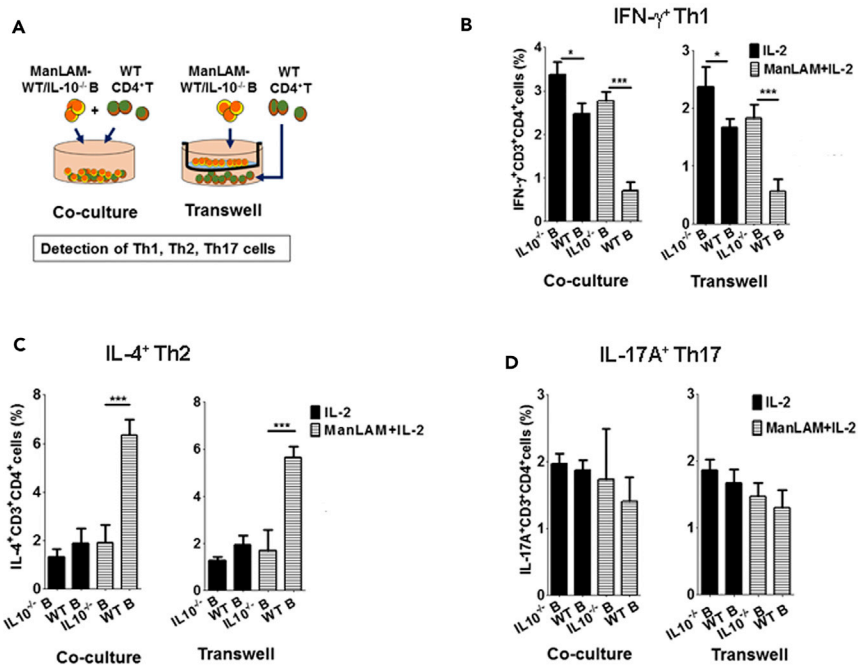

Figure 6. ManLAM-Induced B10 Cells Inhibit Th1 Polarization, Promote Th2 Polarization, and Have No Effect on Th17 *In Vitro*

Splenic B cells were isolated from WT/IL-10$^{-/-}$ mice and stimulated with Rv ManLAM (10 ng/mL) for 12 hr. Then ManLAM was removed by washing. CD4$^+$ T cells were stimulated with plate-coated anti-CD3 antibody (5 μg/mL) and soluble anti-CD28 antibody (2 μg/mL) and then cultured with the ManLAM-treated B cells for 72 hr.

(A) Schematic diagram.

(B–D) (B) IFN-γ, (C) IL-4, and (D) IL-17A production by CD4$^+$ T cells were analyzed by flow cytometry. (B–D) The cells were cultured in medium containing IL-2. Data are represented as mean ± SD. ***$p < 0.001$, *$p < 0.05$.

See also Figure S6.

were enriched in Kyoto Encyclopedia of Genes and Genomes pathway (FDR ≤ 0.01, Figure S5B). From the above-mentioned analysis, we found that ManLAM-TLR2 interaction markedly caused the changes of chemokine and NF-κB pathway in CD1d^{hi}CD5$^+$ B cells.

The results of hierarchical cluster analysis of gene expression patterns showed that that the mRNA expression of USP40 was upregulated in ManLAM-treated WT CD1d^{hi}CD5$^+$ B cells than the unstimulated control (Figure 5B). USP40 is a member of the ubiquitin proteasome system. The system is responsible for protein ubiquitination and proteasomal degradation. Our results from quantitative reverse-transcriptase PCR and immunoblotting analysis further confirmed that the mRNA and protein expression levels of USP40 were also greatly upregulated in the WT B cells compared with the TLR2$^{-/-}$ B cell groups when these cells were stimulated with ManLAM/Pam3CSK4 (Figure S5C). We constructed USP40-shRNA to silence the USP40 expression in B cells (Figures S5D and S5E). Knockdown of USP40 significantly decreased ManLAM/Pam3CSK4-induced IL-10 production by WT B cells, whereas IL-10 production by USP40-silenced TLR2$^{-/-}$ B cells was not reduced compared with scramble RNA-treated TLR2$^{-/-}$ B cells upon stimulation with ManLAM (Figures 5C, 5D, and S5F). Our data suggest that ManLAM induces IL-10 production in B cells via TLR2 and USP40. ManLAM-TLR2 induces USP40 increase, which positively regulated the IL-10 production in B cells (Figures 5B–5D and S5C–S5F).

ManLAM-Induced B10 Cells Inhibit Th1 Polarization, Promote Th2 Polarization, and Have No Effect on Th17 Cells *In Vitro* and *In Vivo*

Next, we investigated the effects of ManLAM-induced B10 cells on CD4$^+$ T cell polarization. CD4$^+$ T cells were co-cultured with ManLAM-treated WT/IL-10$^{-/-}$ B cells. The production of interferon (IFN)-γ, IL-4, and IL-17A of CD4$^+$ T cells was then determined (Figure 6A). Compared with the ManLAM-treated IL-10$^{-/-}$ B cells group, IFN-γ-producing CD4$^+$ T cells were significantly decreased when the cells were co-cultured

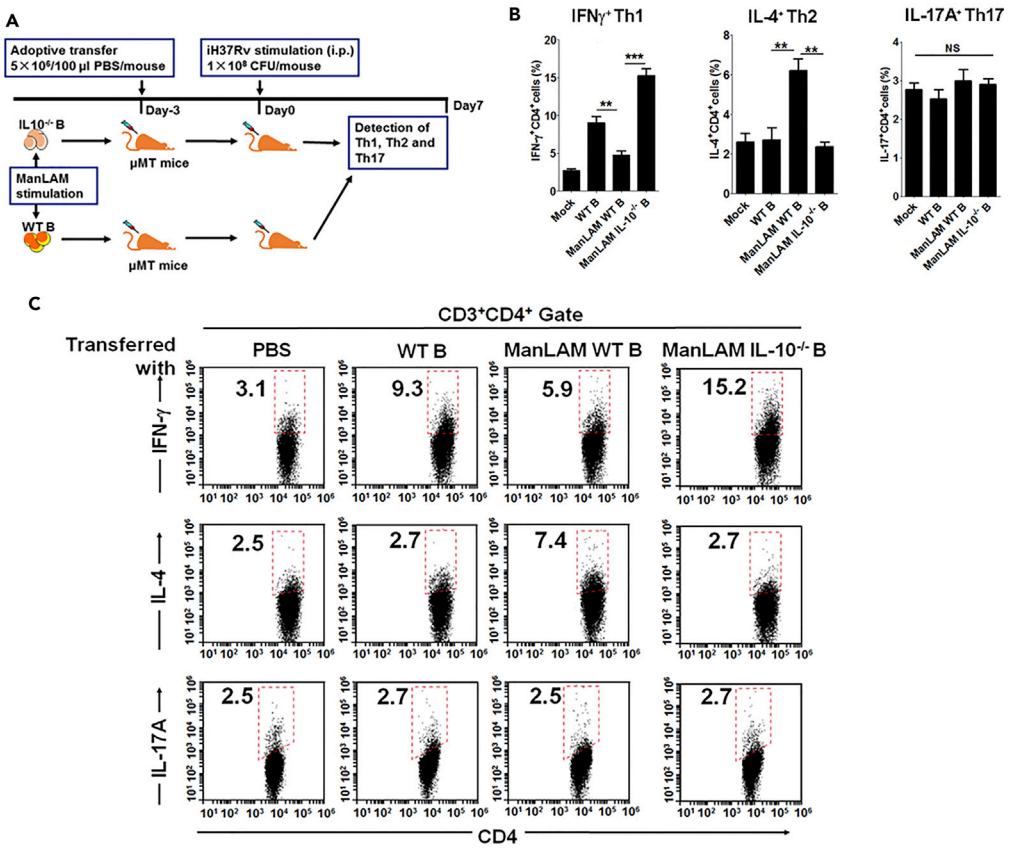

Figure 7. ManLAM-Induced B10 Cells Inhibit Th1 Polarization, Promote Th2 Polarization, and Have No Effect on Th17 *In Vivo*

(A–C) ManLAM-treated WT/IL-10$^{-/-}$ B cells were adoptively transferred into μMT mice. The mice were primed by iH37Rv. (A) Schematic diagram. (B) IFN-γ, IL-4, and IL-17A production by splenic CD4$^+$ T cells were determined by flow cytometry. Data were shown as means ± SD (n = 6). ***p < 0.001, **p < 0.01; NS, not significant. (C) Representative dot plots.

with ManLAM-treated WT B cells, whereas IL-4-producing CD4$^+$ T cells were markedly increased in the ManLAM-treated WT B cell group (Figures 6B, 6C, S6A, and S6B). There were no significant differences in IL-17A-producing CD4$^+$ T cells among the groups (Figures 6D and S6C). Similar results were obtained in transwell assays (Figures 6B–6D and S6A–S6C). The upper chambers in transwell plates with a pore size of 0.4 μm prevented direct cell-cell contact but allowed the exchange of soluble factors (Noack et al., 2016). These results indicate that IL-10 secreted by ManLAM-treated B cells inhibits Th1 polarization, but promotes Th2 polarization, and has no effect on Th17 cells *in vitro*.

To assess the regulation of CD4$^+$ T cell polarization *in vivo* by ManLAM-induced B10 cells, we used the iH37Rv-primed mouse model. ManLAM-treated WT or IL-10$^{-/-}$ B cells were adoptively transferred into B cell-deficient μMT mice. The recipient mice were primed with iH37Rv. The polarization of splenic CD4$^+$ T cells was evaluated after 7 days of adoptive transfer (Figure 7A). Consistent with the *in vitro* results, the transferred ManLAM-treated WT B cells induced a significant decrease in splenic IFN-γ-producing CD4$^+$ T cells, but an increase in IL-4-producing CD4$^+$ T cells compared with the ManLAM-treated IL-10$^{-/-}$ B cell group (Figures 7B and 7C). Adoptive transfer of ManLAM-treated WT B cells did not change the percentage of IL-17A-producing CD4$^+$ T cells (Figures 7B and 7C). These findings strongly suggest that ManLAM-induced B10 cells inhibit Th1 polarization, promote Th2 polarization, and have no effect on Th17 cells *in vitro* and *in vivo*.

ManLAM-Induced B10 Cells Increase Susceptibility to Mtb Infection in Mice

Next we used WT BCG infection model to explore the role of ManLAM-induced B10. Rag2$^{-/-}$ mice were adoptively transferred with ManLAM-treated WT/IL-10$^{-/-}$ B cells plus CD4$^+$ T cells and infected

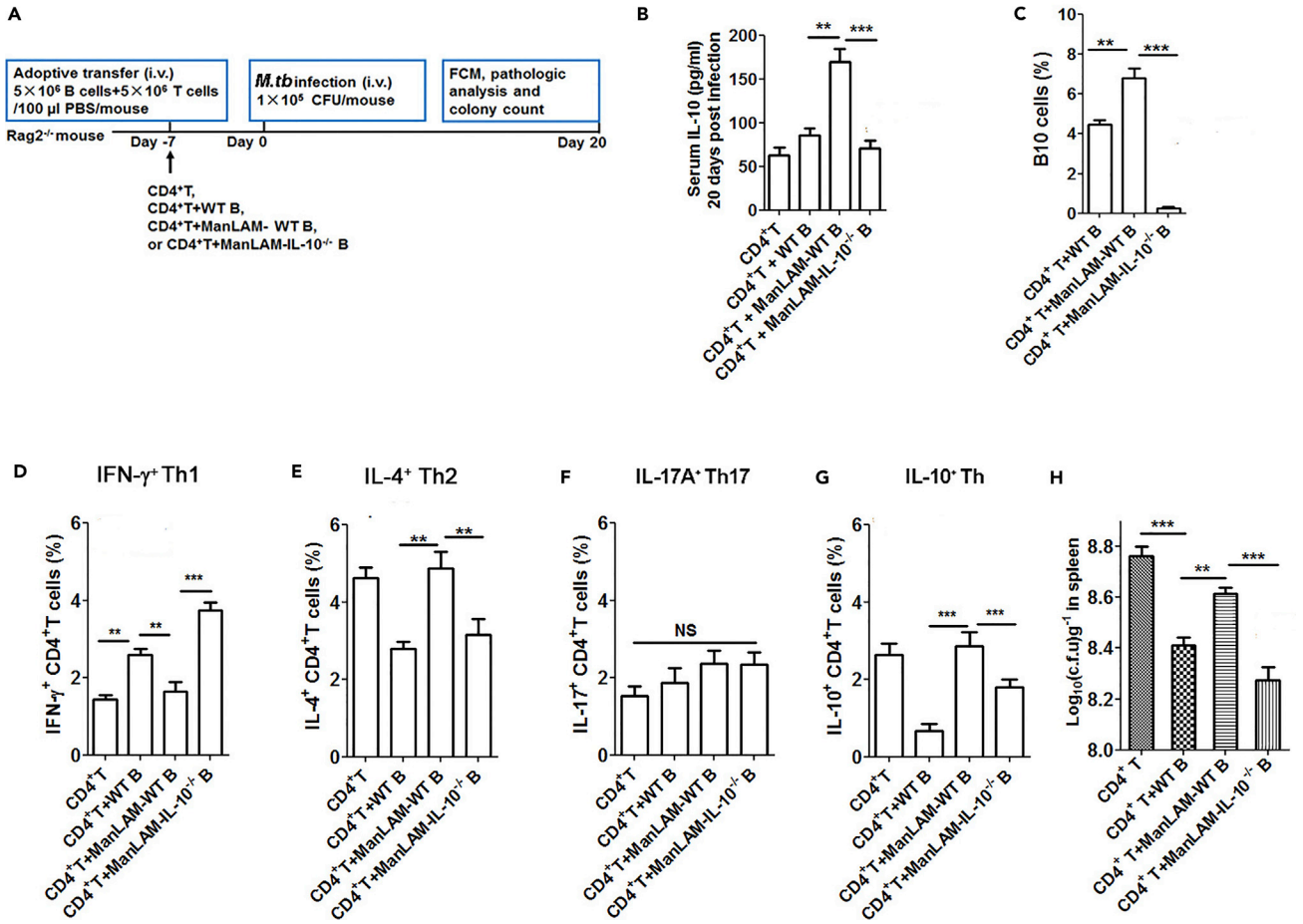

Figure 8. ManLAM-Induced B10 Cells Increase Susceptibility to Mtb Infection in Mice

ManLAM-treated WT/IL-10$^{-/-}$ B cells were adoptively transferred into Rag2$^{-/-}$ mice. The mice were infected with BCG.

(A) Schematic diagram.

(B) After 20 days of infection, serum IL-10 level was determined by ELISA. Data are represented as mean ± SD. ***$p < 0.001$, **$p < 0.01$.

(C–G) Splenic B10 cells and cytokines produced by splenic CD4$^+$ T cells were determined by flow cytometry. (C) B10 cells; (D) IFN-γ, (E) IL-4, (F) IL-17A, and (G) IL-10 production by CD4$^+$ T cells. Data are represented as mean ± SD. ***$p < 0.001$, **$p < 0.01$.

(H) CFU assay in spleens. Data are represented as mean ± SD. ***$p < 0.001$, **$p < 0.01$.

See also Figures S7 and S8.

(intravenously [i.v.]) with BCG (Figure 8A). Usually a low-dose aerosol of Mtb (approximately 50–100 colony-forming unit [CFU] in mice) causes chronic infection (Upton et al., 2015), whereas a high dose (>10^2 CFU, aerosol/i.v.) causes acute infection (Mayer-Barber et al., 2014; Aggarwal et al., 2017; Das et al., 2013). Because mice that inhaled 1 × 10^2–1×10^4 or i.v. administered 1 × 10^5–2 × 10^6 CFU of Mtb (Mtb H37Rv, H37Ra, or BCG) showed similar pathological changes in acute infection model (Mayer-Barber et al., 2014; Aggarwal et al., 2017; Das et al., 2013; Stüve et al., 2018), 1 × 10^5 CFU of Mtb/mouse (i.v. infection) was used in our mouse model. After 20 days of infection, transferred CD19$^+$ B cells and CD3$^+$CD4$^+$ T cells were observed in the Rag2$^{-/-}$ mice (Figure S7A). Serum IL-10 and B10 cells were increased in the mice transferred with ManLAM-treated WT B cells compared with other groups (Figures 8B, 8C, and S7B). These results demonstrated that ManLAM-treated B cells secreted IL-10 and contributed to increased serum levels of IL-10.

Consistent with the above-mentioned results, transfer of ManLAM-treated WT B cells reduced IFN-γ production, but promoted IL-4 production by splenic CD4$^+$ T cells compared with the WT B cell group and ManLAM-treated IL-10$^{-/-}$ B cell group, whereas IL-17A production by CD4$^+$ T cells did not significantly change among all groups during BCG infection (Figures 8D–8F and S7C). Moreover, the increased level of IL-10-producing CD4$^+$ T cells was observed in ManLAM-treated WT B cell group (Figures 8G and S7C).

BCG CFUs in spleens were significantly increased in the ManLAM-treated WT B group compared with WT B cell group and ManLAM-treated IL-10$^{-/-}$ B cell group (Figure 8H). These results clearly demonstrated that ManLAM-induced B10 cells increased susceptibility to BCG infection and facilitated the bacterial survival in mice.

Finally, we assessed the roles of the ManLAM-induced B10 cells during virulent Mtb H37Rv infection. Rag2$^{-/-}$ mice were adoptively transferred with ManLAM-treated WT/IL-10$^{-/-}$ B cells plus CD4^{+} T cells and infected (i.v.) with virulent Mtb H37Rv (Figure S8A). After 20 days of infection, the level of serum IL-10 was greatly elevated (Figure S8B), and Mtb H37Rv CFUs in both lung and spleen tissues were also higher in the ManLAM-treated WT B group compared with the ManLAM-treated IL10$^{-/-}$ B group (Figures S8C and S8D upper panel). In PBS-transferred group, Rag2$^{-/-}$ mice had no mature T and B cells, so the highest Mtb H37Rv CFUs were found in this PBS group (Figures S8C and S8D upper panel). Compared with the ManLAM-treated IL-10$^{-/-}$ B group, histopathological analysis of alveolar tissue from the ManLAM-treated WT B and PBS groups showed larger amount of lymphocyte infiltration (Figure S8D lower panel). Histological examination of splenic tissues demonstrated that white pulp and red pulp in spleen tissues from the ManLAM-treated WT B and PBS groups were more completely disorganized, with many basophilic granules and necrotic cellular debris, compared with the ManLAM-treated IL-10$^{-/-}$ B group (Figure S8D lower panel). These findings confirmed that ManLAM-induced B10 cells facilitated mycobacterial survival in the mice.

DISCUSSION

Some evidence has shown that B cells favor anti-TB immunity and prolong mouse survival (Kozakiewicz et al., 2013; Maglione et al., 2007). Distinct B cell subsets might play different roles in anti-TB immunity. B10 cells, a subtype of Bregs, have been rarely reported in Mtb infection. It has been reported that TLR2/TLR4 ligands from Freund's adjuvant induce B10 cells (Lampropoulou et al., 2008). Freund's adjuvant from BCG components may contain ManLAM. We demonstrated that ManLAM and Mtb themselves induced B10 cells in a TLR2/MyD88-dependent manner, which was consistent with the previous study (Lampropoulou et al., 2008).

ManLAM has been reported to be released from the metabolically active or degrading bacterial cells and shed into body fluid (like sputum, blood, or urine) during TB infection, which appears to be present only in people with ATB disease (Paris et al., 2017). Based on this character, ManLAM has been used as a target for TB diagnosis (Pandie et al., 2016; Gupta-Wright et al., 2018). Therefore, we could measure serum ManLAM concentrations in patients with ATB (Figure 1D), although the enzyme-linked oligonucleotide assay used here could not distinguish between ManLAM and whole bacteria.

Several studies reported that IL-10 was also produced by human CD4^{+} T cells, DCs, and macrophages in patients with ATB (Kumar et al., 2015; Redford et al., 2011). In mouse TB models, IL-10 production was mainly from monocytes in the mouse lung after Mtb infection (Moreira-Teixeira et al., 2017). A small proportion cells (30%–50% in total IL-10^{+} cells), including DCs, macrophages, T cells, and B cells, produced IL-10 (Moreira-Teixeira et al., 2017). Here, we identified that increased B10 cells played an important role during Mtb infection by hindering Th1 immunity. A comparison of the functions among various types of IL-10^{+} cells in TB infection models may need to be further investigated.

The frequencies of various types of IL-10^{+} cells change dynamically during Mtb infection. Previous studies from our group and those of others have shown about 5%–40% IL-10^{+} DCs (in total DCs) and 10%–30% IL-10^{+} macrophages (in total macrophages) induced by Mtb in mice (Moreira-Teixeira et al., 2017; Sun et al., 2016). Here, we measured about 4.0% $\pm$ 0.3% B10 cells in patients with ATB and 6%–8% B10 in Mtb infected mice (Figures 1C and 2G–2I). It has been reported that the peak level of proportion of IL-10^{+} DCs/macrophages reached within 28 days of Mtb infection and then gradually decreased (Moreira-Teixeira et al., 2017). The proportion of B10 cells was about 10% at day 7 post-infection, sharply decreased at day 14, and then increased 2-fold during chronic Mtb infection (days 21–57) (Moreira-Teixeira et al., 2017). The B10 level (10%–12% in total IL-10^{+} cells) was similar to the level of IL-10^{+} DCs and macrophages at day 57 post-infection (Moreira-Teixeira et al., 2017). We speculate that levels of different IL-10-producing cells might be changed with the progress of infection. The effect of *in vivo* B10 cell depletion in infected WT mice will need to be detected in future studies to assess the dynamic effects of B10 and other IL-10^{+} cells during Mtb infection.

We found that IL-10 expression by B cells reached a peak at 12 hr and then decreased after ManLAM stimulation (Figures 2D and S1F). The reasons might be the rapid induction and degradation of IL-10 mRNA in the activation of TLR2 signaling triggered by microbial molecules (Gabrysova et al., 2014; Eixeira-Coelho et al., 2014). We also found that IL-10 production in B cells first increased (1–10 ng/mL of ManLAM) and then decreased as the concentrations further increased (>10 ng/mL of ManLAM) (Figures 2E and S1G). Unlike protein antigens, the structure of the aliphatic and carbohydrate chains are diverse and complex as the concentrations of these molecules increased (Holderness et al., 2011; Jagger et al., 2002). Therefore, the increased concentration of ManLAM would not always induce an enhancement of cytokine production by immune cells. Moreover, ManLAM can be recognized by CD44 on the macrophages, which may downregulate IL-10 production (Sun et al., 2016). Whether ManLAM-CD44 interaction in B cells and ManLAM-TLR2 interaction in macrophages have effects on IL-10 production needs to be further investigated.

As shown in the left panel of Figure 2E, at higher concentrations of ManLAM (>10 ng/mL), the IL-10 level tended to decrease but was still significantly higher than that in the control group. These results indicate that a wide range of ManLAM concentrations (from 0 to 10 μg/mL) induced B cells to produce IL-10, contributing to elevate total serum IL-10 level in patients with ATB. As shown in Figure 1D, the average concentration of ManLAM in 30 patients with ATB was 156.1 ng/mL (95% CI = 95.5–216.6 ng/mL). The above range of ManLAM concentrations in patients with ATB could induce B cells to produce IL-10, which might have biological function in patients with ATB.

As shown in Figures 2G and 2H, the percentage of splenic B10 cells from non-immunized mice (PBS group) was approximately 2%, which was consistent with a previous report (Matsushita and Tedder, 2011). Our present data showed that approximately 6%–8% of B10 cells were induced by immunization with ManLAM/iH37Rv/iBCG *in vivo*, in which the frequency of B10 cells was similar to that in LPS-stimulated mice (Maseda et al., 2012). To the best of our knowledge, our study is the first report to describe the numbers of B10 cells induced by ManLAM/iH37Rv/iBCG in mice (Figures 2G and 2H).

TLR ligands binding various TLRs can induce IL-10 production by human and murine B cells (Mauri and Bosma, 2012; Mizoguchi and Bhan, 2006). Here we reported that ManLAM induced B10 cells via TLR2-mediated signaling. TLR2 has been implicated as a major signaling receptor that binds to lipoarabinomannan (Osanya et al., 2011). MR knockdown could not cause a significant reduction of IL-10 in $TLR2^{-/-}$ B cells treated with ManLAM (Figure 3B), and knockdown of MR in $TLR2^{-/-}$ B cells had fairly limited effects on ManLAM signaling (Figure S4G). These results indicated that ManLAM-MR binding only had a minor effect on triggering IL-10 production by B cells. As shown in Figures 3C–3E, recognition by TLR2 was the predominant mechanism of IL-10 production by ManLAM-treated B cells.

K63-linked ubiquitination of NEMO was observed in the ManLAM-treated B cells (Figure 5A). NEMO ubiquitination-mediated NF-κB activation regulates many viral and bacterial infections (Ashida et al., 2010; Fang et al., 2017). It has been reported that Mtb PtpA, a secreted tyrosine phosphatase, directly blocks host TAB3 from binding K63-linked ubiquitin chains, suppresses NF-κB activation, and contributes to immune evasion (Wang et al., 2015). In the current study, we demonstrated that ManLAM-induced IL-10 production by B cells was associated with the promotion of NEMO K63 ubiquitination and NF-κB activation. Consistent with our study, other groups have also reported that ManLAM induces IL-10 and COX2 expression by activating TLR2/NF-κB signaling in macrophages and DCs (Kumar et al., 2013; Rajaram et al., 2010; Vergne et al., 2014).

B10 cells have been implicated in the Th1 to Th2 shift during *Leishmania* and *Salmonella typhimurium* infection in mice (Neves et al., 2010; Ronet et al., 2010). It is widely accepted that the dominant protective response in TB is a Th1-type response. Th1 cytokine IFN-γ is a cytokine that plays a critical role in resistance to Mtb infection (Fenton et al., 1997), whereas Th2 cytokine IL-4 facilitates Mtb escape (Rook et al., 2004). In our study, the results from the μMT mice primed by iH37Rv and $Rag2^{-/-}$ mice infected with BCG experiments showed that the IL-4 production in $CD4^{+}$T cells were increased (Figures 7B, 7C, 8E, and S7C). Greatly increased Th1 development was demonstrated in co-culture and transwell experiments using $IL\text{-}10^{-/-}$ B cells *in vitro* (Figure 6B), and *in vivo* adoptive transfer experiments (Figures 7B, 7C, 8D, and S7C). These results indicated that ManLAM hindered Th1 development/function during Mtb infection via IL-10 from B10 and possibly from Th2 cells. Consistently, Schierloh et al. reported that human B cells isolated from the

pleural fluid of patients with TB produced IL-10 upon stimulation with γ-irradiated Mt and that these B cells diminished *in vitro* Mtb-induced IFN-γ production by T cells and natural killer cells in an IL-10-dependent manner (Schierloh et al., 2014).

It has been reported that IL-10 from B cells downregulates T-bet activation and IFN-γ production in Th cells (Flores-Borja et al., 2013). We also confirmed that IL-10 produced by ManLAM-treated B cells inhibited the development of Th1 IFN-γ^+ $CD4^+$ T cells, but promoted the development Th2 IL-4^+CD4^+T cells (Figures 7 and 8). IFN-γ and IL-4 are signature cytokines for Th1 and Th2 cells, respectively, so we measured these cytokines. The effects of ManLAM-induced B10 cells on the expression of Th1/2-related transcription factors (such as T-bet and GATA3) and other Th1-type cytokines (such as IL-12 and tumor necrosis factor-α) need to be clarified in the future.

In the present study, we found ManLAM-TLR2 induced the IL-10 production in B cells due in part to intracellular increased USP40. We found that USP40, a member of the ubiquitin proteasome system, was involved in the upregulation of IL-10 production by ManLAM-treated B cells (Figures 5B–5D and S5C–S5F). However, molecular interactions with USP40, and the process of USP40-mediated upregulation of IL-10 production in ManLAM-treated B cells, require elucidation in further studies. Second, several studies have reported that NF-κB is an important mediator involved in the production of both anti- and pro-inflammatory cytokines in B cells (Lee et al., 2017; Walsh et al., 2015). Our study showed that ManLAM activated NF-κB pathway and induced anti-inflammatory cytokine IL-10 in B cells. These indicate that other inflammatory cytokines might be induced by ManLAM-treated B cells via NF-κB signaling.

Recently, Bénard et al. reported that type I IFN produced by Mtb-stimulated B cells favors macrophage polarization toward a regulatory/anti-inflammatory phenotype during Mtb infection (Bénard et al., 2018). In addition, they also found a modest increase of IL-10 mRNA in B cells isolated from the lungs of Mtb-infected WT mice, which is consistent with our results. In our current study, we demonstrate that ManLAM induces IL-10 production of B cells, which hinders the Th1 response. We hypothesize that Mtb may negatively regulate immune response via B10 cells. Whether the B10 cells induced by ManLAM are polyfunctional for the production of type I IFN should be investigated in the future.

B cells are the dominant antigen-presenting cells that activate naive $CD4^+$ T cells upon immunization with a viral antigen (Hong et al., 2018). Besides antigen presentation, B cells also have multifunction, including antibody production and cytokine secretion, and have effects on the T cell activation during Mtb infection (Chan et al., 2014). Thus, when WT B cells were adoptively transferred into μMT mice, the transferred WT B cells promoted Th1 cell activation upon stimulation with iH37Rv (Figures 7B and 8D). More importantly, peak levels of IFNγ^+CD4^+ T cells were detected when ManLAM-treated IL-$10^{-/-}$ B cells were adoptively transferred (Figures 7B and 8D). The levels appear to be significantly higher than those observed when WT B cells are transferred. IL-$10^{-/-}$ B cells do not produce IL-10 for suppressing Th1 polarization, so these IL-$10^{-/-}$ B cells induce higher level of IFNγ^+CD4^+ T cells compared with the WT B cells group. These results clearly demonstrate that ManLAM hinders Th1 development/function during Mtb infection via IL-10 from B cells. Moreover, ManLAM-treated B cells might also be partially involved in anti-TB immune response like antigen presentation.

Collectively, we report a new immunoregulation mechanism in which Mtb ManLAM induced-B10 cells negatively regulate host anti-TB cellular immunity. Our data showed that Mtb ManLAM induced B10 cells with $CD5^+$ B1a subset. Molecular mechanism analysis reveals that the interaction of ManLAM and TLR2 induces IL-10 production by B cells mainly via the TLR2/MyD88/PI3K/AKT/AP-1 and NEMO K63 ubiquitination NF-κB signaling pathways, and increased USP40. ManLAM-induced B10 cells hinder Th1 responses, promote Th2 polarization, and have no effect on Th17 cells. ManLAM-induced B10 cells increase susceptibility to Mtb infection in mice. Our findings will help to understand the interaction between B cells and Mtb ManLAM and highlight the ManLAM-mediated B cells' immunomodulatory functions.

Limitations of the Study

The overall cytokine expressions, including the production of type I and type II IFNs, as well as multiple functions (like antigen presentation) of ManLAM-treated B10 cells have not been detected and are worth investigating in the future.

METHODS

All methods can be found in the accompanying Transparent Methods supplemental file.

DATA AND SOFTWARE AVAILABILITY

RNA-seq data reported in this study has been submitted to the NCBI SRA: PRJNA505400 (https://submit.ncbi.nlm.nih.gov/subs/sra/)

SUPPLEMENTAL INFORMATION

Supplemental Information includes Transparent Methods and eight figures and can be found with this article online at https://doi.org/10.1016/j.isci.2018.11.039.

ACKNOWLEDGMENTS

We acknowledge Drs. Hongbing Shu and Yanyi Wang (Wuhan University, Wuhan, China) for providing plasmids encoding NEMO, WT ubiquitin (H-Ub), ubiquitin mutant H-Ub (K48), and H-Ub (K63). We acknowledge Dr. Youchun Wang (National Institutes for Food and Drug Control, Beijing, China) for providing $Rag2^{-/-}$ mice and Dr. Hai Qi (University of Tsinghua, Beijing, China) for providing μMT mice.

This work was supported by grants from the National Key R&D Program of China http://www.most.gov.cn (2018YFA0507603 to X.-L.Z.), National Natural Science Foundation of China http://www.nsfc.gov.cn (31221061 to X.-L.Z., 31370197 to X.-L.Z., 21572173 to X.-L.Z., 81471910 to Q.P., and 31770145 to Q.P.), National Science and Technology Major Project http://www.most.gov.cn (2017ZX10201301-006 to X.-L.Z., 2012ZX10003002-015 to X.-L.Z.), National Outstanding Youth Foundation of China http://www.nsfc.gov.cn (81025008 to X.-L.Z.), the Major Projects of Technological Innovation of Hubei Province http://www.hbstd.gov.cn (2016ACA150 to X.-L.Z.), Natural Science Foundation Project of Hubei Province http://www.hbstd.gov.cn (2016CFA062 to X.-L.Z.), the Outstanding Youth Foundation of Hubei Province http://www.hbstd.gov.cn (2018CFA037 to Q.P.), and the Wuhan Youth Science and Technology Chenguang Plan http://www.whst.gov.cn (2016070204010127 to Q.P.). The funders had no role in study design, data collection and analysis, decision to publish, or preparation of the manuscript.

AUTHOR CONTRIBUTIONS

X.-L.Z. and Q.P. designed the research; X.-L.Z. and Q.P. supervised the research; C.Y. and Z.-L.Q. conducted the experiments; C.Y., Q.P., and X.-L.Z. wrote the manuscript and X.-L.Z. revised the manuscript; Q.L., W.L., X.-L.T., and C.H. helped with the experiments.

DECLARATION OF INTERESTS

The authors declare no competing interests.

Received: August 30, 2018
Revised: November 8, 2018
Accepted: November 28, 2018
Published: January 25, 2019

REFERENCES

Achkar, J.M., Chan, J., and Casadevall, A. (2015). B cells and antibodies in the defense against *Mycobacterium tuberculosis* infection. Immunol. Rev. *264*, 167–181.

Aggarwal, A., Parai, M.K., Shetty, N., Wallis, D., Woolhiser, L., Hastings, C., Dutta, N.K., Galaviz, S., Dhakal, R.C., Shrestha, R., et al. (2017). Development of a novel lead that targets *M. tuberculosis* polyketide synthase 13. Cell *170*, 249–259.e25.

Ariizumi, K., Shen, G.L., Shikano, S., Ritter, R., 3rd, Zukas, P., Edelbaum, D., Morita, A., and Takashima, A. (2000). Cloning of a second dendritic cell-associated C-type lectin (dectin-2) and its alternatively spliced isoforms. J. Biol. Chem. *275*, 11957–11963.

Ashida, H., Kim, M., Schmidt-Supprian, M., Ma, A., Ogawa, M., and Sasakawa, C. (2010). A bacterial E3 ubiquitin ligase IpaH9.8 targets NEMO/IKKgamma to dampen the host NF-kappaB-mediated inflammatory response. Nat. Cell Biol. *12*, 66–73.

Bénard, A., Sakwa, I., Schierloh, P., Colom, A., Mercier, I., Tailleux, L., Jouneau, L., Boudinot, P., Al-Saati, T., Lang, R., et al. (2018). B cells producing type I IFN modulate macrophage polarization in tuberculosis. Am. J. Respir. Crit. Care Med. *197*, 801–813.

Bod, L., Douguet, L., Auffray, C., Lengagne, R., Bekkat, F., Rondeau, E., Molinier-Frenkel, V., Castellano, F., Richard, Y., and Prévost-Blondel, A. (2018). IL-4-induced gene 1: a negative immune checkpoint controlling B cell differentiation and activation. J. Immunol. *200*, 1027–1038.

Chan, J., Mehta, S., Bharrhan, S., Chen, Y., Achkar, J.M., Casadevall, A., and Flynn, J. (2014). The role of B cells and humoral immunity in *Mycobacterium tuberculosis* infection. Semin. Immunol. *26*, 588–600.

Das, A., Ellis, G., Pallant, C., Lopes, A.R., Khanna, P., Peppa, D., Chen, A., Blair, P., Dusheiko, G., Gill, U., et al. (2012). IL-10-producing regulatory B cells in the pathogenesis of chronic hepatitis B virus infection. J. Immunol. *189*, 3925–3935.

Das, B., Kashino, S.S., Pulu, I., Kalita, D., Swami, V., Yeger, H., Felsher, D.W., and Campos-Neto, A. (2013). CD271(+) bone marrow mesenchymal stem cells may provide a niche for dormant *Mycobacterium tuberculosis*. Sci. Transl. Med. *5*, 170ra13.

Ding, Q., Yeung, M., Camirand, G., Zeng, Q., Akiba, H., Yagita, H., Chalasani, G., Sayegh, M.H., Najafian, N., and Rothstein, D.M. (2011). Regulatory B cells are identified by expression of TIM-1 and can be induced through TIM-1 ligation to promote tolerance in mice. J. Clin. Invest *121*, 3645–3656.

Du, Q., Huang, Y., Wang, T., Zhang, X., Chen, Y., Cui, B., Li, D., Zhao, X., Zhang, W., Chang, L., and Tong, D. (2016). Porcine circovirus type 2 activates PI3K/Akt and p38 MAPK pathways to promote interleukin-10 production in macrophages via Cap interaction of gC1qR. Oncotarget *7*, 17492–17507.

Eixeira-Coelho, M., Guedes, J., Ferreirinha, P., Howes, A., Pedrosa, J., Rodrigues, F., Lai, W.S., Blackshear, P.J., O'Garra, A., Castro, A.G., Saraiva, M., et al. (2014). Differential post-transcriptional regulation of IL-10 by TLR2 and TLR4-activated macrophages. Eur. J. Immunol. *44*, 856–866.

Fang, R., Jiang, Q., Zhou, X., Wang, C., Guan, Y., Tao, J., Xi, J., Feng, J.M., and Jiang, Z. (2017). MAVS activates TBK1 and IKKepsilon through TRAFs in NEMO dependent and independent manner. PLoS Pathog. *13*, e1006720.

Fenton, M.J., Vermeulen, M.W., Kim, S., Burdick, M., Strieter, R.M., and Kornfeld, H. (1997). Induction of gamma interferon production in human alveolar macrophages by *Mycobacterium tuberculosis*. Infect. Immun. *65*, 5149–5156.

Ferrier, D. (2017). Lippincott illustrated reviews: biochemistry. In UNIT I, Protein Structure and Function, Chapter2 Protein Structure, S. Magee and C. Fahey, eds. (Wolters Kluwer), pp. 13–24.

Flores-Borja, F., Bosma, A., Ng, D., Reddy, V., Ehrenstein, M.R., Isenberg, D.A., and Mauri, C. (2013). CD19+CD24hiCD38hi B cells maintain regulatory T cells while limiting TH1 and TH17 differentiation. Sci. Transl. Med. *5*, 173ra23.

Fratti, R.A., Chua, J., Vergne, I., and Deretic, V. (2003). *Mycobacterium tuberculosis* glycosylated phosphatidylinositol causes phagosome maturation arrest. Proc. Natl. Acad. Sci. U S A *100*, 5437–5442.

Gabrysova, L., Howes, A., Saraiva, M., and O'Garra, A. (2014). The regulation of IL-10 expression. Curr. Top. Microbiol. Immunol. *380*, 157–190.

Gaddis, D.E., Maynard, C.L., Weaver, C.T., Michalek, S.M., and Katz, J. (2013). Role of TLR2-dependent IL-10 production in the inhibition of the initial IFN-gamma T cell response to *Porphyromonas gingivalis*. J. Leukoc. Biol. *93*, 21–31.

Geijtenbeek, T.B., Van Vliet, S.J., Koppel, E.A., Sanchez-Hernandez, M., Vandenbroucke-Grauls, C.M., Appelmelk, B., and Van Kooyk, Y. (2003). *Mycobacteria* target DC-SIGN to suppress dendritic cell function. J. Exp. Med. *197*, 7–17.

Geneva: World Health Organization, Global tuberculosis report 2017. Licence: CC BY-NCSA 3.0 IGO (2017). Available at: http://apps.who.int/medicinedocs/en/m/abstract/Js23360en/.

Gupta-Wright, A., Corbett, E.L., van Oosterhout, J.J., Wilson, D., Grint, D., Alufandika-Moyo, M., Peters, J.A., Chiume, L., Flach, C., Lawn, S.D., and Fielding, K. (2018). Rapid urine-based screening for tuberculosis in HIV-positive patients admitted to hospital in Africa (STAMP): a pragmatic, multicentre, parallel-group, double-blind, randomised controlled trial. Lancet *392*, 292–301.

Hamasur, B., Haile, M., Pawlowski, A., Schroder, U., Kallenius, G., and Svenson, S.B. (2004). A mycobacterial lipoarabinomannan specific monoclonal antibody and its F(ab') fragment prolong survival of mice infected with *Mycobacterium tuberculosis*. Clin. Exp. Immunol. *138*, 30–38.

Hoff, S.T., Salman, A.M., Ruhwald, M., Ravn, P., Brock, I., Elsheikh, N., Andersen, P., and Agger, E.M. (2015). Human B cells produce chemokine CXCL10 in the presence of *Mycobacterium tuberculosis* specific T cells. Tuberculosis (Edinb.) *95*, 40–47.

Holderness, J., Schepetkin, I.A., Freedman, B., Kirpotina, L.N., Quinn, M.T., Hedges, J.F., and Jutila, M.A. (2011). Polysaccharides isolated from Acai fruit induce innate immune responses. PLoS One *6*, e17301.

Hong, S., Zhang, Z., Liu, H., Tian, M., Zhu, X., Zhang, Z., Wang, W., Zhou, X., Zhang, F., Ge, Q., et al. (2018). B cells are the dominant antigen-presenting cells that activate naive CD4+ T cells upon immunization with a virus-derived nanoparticle antigen. Immunity *49*, 695–708.e4.

Horikawa, M., Weimer, E.T., DiLillo, D.J., Venturi, G.M., Spolski, R., Leonard, W.J., Heise, M.T., and Tedder, T.F. (2013). Regulatory B cell (B10 Cell) expansion during *Listeria* infection governs innate and cellular immune responses in mice. J. Immunol. *190*, 1158–1168.

Hu, X., Paik, P.K., Chen, J., Yarilina, A., Kockeritz, L., Lu, T.T., Woodgett, J.R., and Ivashkiv, L.B. (2006). IFN-gamma suppresses IL-10 production and synergizes with TLR2 by regulating GSK3 and CREB/AP-1 proteins. Immunity *24*, 563–574.

Jackson, M. (2014). The mycobacterial cell envelope-lipids. Cold Spring Harb. Perspect. Med. *4*, a021105.

Jagger, M.P., Huo, Z., and Riches, P.G. (2002). Inflammatory cytokine (interleukin 6 and tumour necrosis factor alpha) release in a human whole blood system in response to *Streptococcus pneumoniae* serotype 14 and its capsular polysaccharide. Clin. Exp. Immunol. *130*, 467–474.

Karray, S., DeFrance, T., Merle-Béral, H., Banchereau, J., Debré, P., and Galanaud, P. (1988). Interleukin 4 counteracts the interleukin 2-induced proliferation of monoclonal B cells. J. Exp. Med. *168*, 85–94.

Kishimoto, T. (1985). Factors affecting B-cell growth and differentiation. Annu. Rev. Immunol. *3*, 133–157.

Kozakiewicz, L., Chen, Y., Xu, J., Wang, Y., Dunussi-Joannopoulos, K., Ou, Q., Flynn, J.L., Porcelli, S.A., Jacobs, W.R., Jr., and Chan, J. (2013). B cells regulate neutrophilia during *Mycobacterium tuberculosis* infection and BCG vaccination by modulating the interleukin-17 response. PLoS Pathog. *9*, e1003472.

Kumar, N.P., Moideen, K., Banurekha, V.V., Nair, D., Sridhar, R., Nutman, T.B., and Babu, S. (2015). IL-27 and TGFβ mediated expansion of Th1 and adaptive regulatory T cells expressing IL-10 correlates with bacterial burden and disease severity in pulmonary tuberculosis. Immun. Inflamm. Dis. *3*, 289–299.

Kumar, S., Naqvi, R.A., Bhat, A.A., Rani, R., Ali, R., Agnihotri, A., Khanna, N., and Rao, D.N. (2013). IL-10 production from dendritic cells is associated with DC SIGN in human leprosy. Immunobiology *218*, 1488–1496.

Lampropoulou, V., Hoehlig, K., Roch, T., Neves, P., Calderon Gomez, E., Sweenie, C.H., Hao, Y., Freitas, A.A., Steinhoff, U., Anderton, S.M., and Fillatreau, S. (2008). TLR-activated B cells suppress T cell-mediated autoimmunity. J. Immunol. *180*, 4763–4773.

Lee, M.B., Lee, J.H., Hong, S.H., You, J.S., Nam, S.T., Kim, H.W., Park, Y.H., Lee, D., Min, K.Y., Park, Y.M., et al. (2017). JQ1, a BET inhibitor, controls TLR4-induced IL-10 production in regulatory B cells by BRD4-NF-kappaB axis. BMB Rep. *50*, 640–646.

Liu, B.S., Cao, Y., Huizinga, T.W., Hafler, D.A., and Toes, R.E. (2014a). TLR-mediated STAT3 and ERK activation controls IL-10 secretion by human B cells. Eur. J. Immunol. *44*, 2121–2129.

Liu, J., Zhan, W., Kim, C.J., Clayton, K., Zhao, H., Lee, E., Cao, J.C., Ziegler, B., Gregor, A., Yue, F.Y., et al. (2014b). IL-10-producing B cells are induced early in HIV-1 infection and suppress HIV-1-specific T cell responses. PLoS One *9*, e89236.

Lopez-Castejon, G., and Edelmann, M.J. (2016). Deubiquitinases: novel therapeutic targets in immune surveillance? Mediators Inflamm. *2016*, 3481371.

Maglione, P.J., Xu, J., and Chan, J. (2007). B cells moderate inflammatory progression and enhance bacterial containment upon pulmonary challenge with *Mycobacterium tuberculosis*. J. Immunol. *178*, 7222–7234.

Mahon, R.N., Sande, O.J., Rojas, R.E., Levine, A.D., Harding, C.V., and Boom, W.H. (2012). *Mycobacterium tuberculosis* ManLAM inhibits T-cell-receptor signaling by interference with ZAP-70, Lck and LAT phosphorylation. Cell. Immunol. *275*, 98–105.

Maseda, D., Smith, S.H., DiLillo, D.J., Bryant, J.M., Candando, K.M., Weaver, C.T., and Tedder, T.F. (2012). Regulatory B10 cells differentiate into antibody-secreting cells after transient IL-10 production in vivo. J. Immunol. *188*, 1036–1048.

Matsushita, T., and Tedder, T.F. (2011). Identifying regulatory B cells (B10 cells) that

produce IL-10 in mice. Methods Mol. Biol. *677*, 99–111.

Mauri, C., and Bosma, A. (2012). Immune regulatory function of B cells. Annu. Rev. Immunol. *30*, 221–241.

Mayer-Barber, K.D., Andrade, B.B., Oland, S.D., Amaral, E.P., Barber, D.L., Gonzales, J., Derrick, S.C., Shi, R., Kumar, N.P., Wei, W., et al. (2014). Host-directed therapy of tuberculosis based on interleukin-1 and type I interferon crosstalk. Nature *511*, 99–103.

Mishra, A.K., Driessen, N.N., Appelmelk, B.J., and Besra, G.S. (2011). Lipoarabinomannan and related glycoconjugates: structure, biogenesis and role in *Mycobacterium tuberculosis* physiology and host-pathogen interaction. FEMS Microbiol. Rev. *35*, 1126–1157.

Mizoguchi, A., and Bhan, A.K. (2006). A case for regulatory B cells. J. Immunol. *176*, 705–710.

Moreira-Teixeira, L., Redford, P.S., Stavropoulos, E., Ghilardi, N., Maynard, C.L., Weaver, C.T., Freitas do Rosário, A.P., Wu, X., Langhorne, J., and O'Garra, A. (2017). T cell-derived IL-10 impairs host resistance to *Mycobacterium tuberculosis* infection. J. Immunol. *199*, 613–623.

Noack, M., Ndongo-Thiam, N., and Miossec, P. (2016). Interaction among activated lymphocytes and mesenchymal cells through podoplanin is critical for a high IL-17 secretion. Arthritis Res. Ther. *18*, 148.

Neves, P., Lampropoulou, V., Calderon-Gomez, E., Roch, T., Stervbo, U., Shen, P., Kühl, A.A., Loddenkemper, C., Haury, M., Nedospasov, S.A., et al. (2010). Signaling via the MyD88 adaptor protein in B cells suppresses protective immunity during Salmonella typhimurium infection. Immunity *33*, 777–790.

Osanya, A., Song, E.H., Metz, K., Shimak, R.M., Boggiatto, P.M., Huffman, E., Johnson, C., Hostetter, J.M., Pohl, N.L., and Petersen, C.A. (2011). Pathogen-derived oligosaccharides improve innate immune response to intracellular parasite infection. Am. J. Pathol. *179*, 1329–1337.

Pandie, S., Peter, J.G., Kerbelker, Z.S., Meldau, R., Theron, G., Govender, U., Ntsekhe, M., Dheda, K., and Mayosi, B.M. (2016). The diagnostic accuracy of pericardial and urinary lipoarabinomannan (LAM) assays in patients with suspected tuberculous pericarditis. Sci. Rep. *6*, 32924.

Pan, Q., Wang, Q., Sun, X., Xia, X., Wu, S., Luo, F., and Zhang, X.L. (2014). Aptamer against mannose-capped lipoarabinomannan inhibits virulent *Mycobacterium tuberculosis* infection in mice and rhesus monkeys. Mol. Ther. *22*, 940–951.

Paris, L., Magni, R., Zaidi, F., Araujo, R., Saini, N., Harpole, M., Coronel, J., Kirwan, D.E., Steinberg, H., Gilman, R.H., et al. (2017). Urine lipoarabinomannan glycan in HIV-negative patients with pulmonary tuberculosis correlates with disease severity. Sci. Transl. Med. *9*, eaal2807.

Rajaram, M.V., Brooks, M.N., Morris, J.D., Torrelles, J.B., Azad, A.K., and Schlesinger, L.S. (2010). *Mycobacterium tuberculosis* activates human macrophage peroxisome proliferator-activated receptor gamma linking mannose receptor recognition to regulation of immune responses. J. Immunol. *185*, 929–942.

Redford, P.S., Murray, P.J., and O'Garra, A. (2011). The role of IL-10 in immune regulation during *M. tuberculosis* infection. Mucosal Immunol. *4*, 261–270.

Richmond, J.M., Lee, J., Green, D.S., Kornfeld, H., and Cruikshank, W.W. (2012). Mannose-capped lipoarabinomannan from *Mycobacterium tuberculosis* preferentially inhibits sphingosine-1-phosphate-induced migration of Th1 cells. J. Immunol. *189*, 5886–5895.

Ronet, C., Hauyon-La Torre, Y., Revaz-Breton, M., Mastelic, B., Tacchini-Cottier, F., Louis, J., and Launois, P. (2010). Regulatory B cells shape the development of Th2 immune responses in BALB/c mice infected with Leishmania major through IL-10 production. J. Immunol. *184*, 886–894.

Rook, G.A., Hernandez-Pando, R., Dheda, K., and Teng Seah, G. (2004). IL-4 in tuberculosis: implications for vaccine design. Trends Immunol. *25*, 483–488.

Saraiva, M., and O'Garra, A. (2010). The regulation of IL-10 production by immune cells. Nat. Rev. Immunol. *10*, 170–181.

Schierloh, P., Landoni, V., Balboa, L., Musella, R.M., Castagnino, J., Morana, E., de Casado, G.C., Palmero, D., and Sasiain, M.C. (2014). Human pleural B-cells regulate IFN-gamma production by local T-cells and NK cells in a *Mycobacterium tuberculosis*-induced delayed hypersensitivity reaction. Clin. Sci. (Lond.) *127*, 391–403.

Soilleux, E.J., Morris, L.S., Leslie, G., Chehimi, J., Luo, Q., Levroney, E., Trowsdale, J., Montaner, L.J., Doms, R.W., Weissman, D., et al. (2002). Constitutive and induced expression of DC-SIGN on dendritic cell and macrophage subpopulations in situ and in vitro. J. Leukoc. Biol. *71*, 445–457.

Stüve, P., Minarrieta, L., Erdmann, H., Arnold-Schrauf, C., Swallow, M., Guderian, M., Krull, F., Hölscher, A., Ghorbani, P., Behrends, J., et al. (2018). De Novo fatty acid synthesis during Mycobacterial infection is a prerequisite for the function of highly proliferative t cells, but not for dendritic cells or macrophages. Front. Immunol. *9*, 495.

Sun, X., Pan, Q., Yuan, C., Wang, Q., Tang, X.L., Ding, K., Zhou, X., and Zhang, X.L. (2016). A single ssDNA aptamer binding to mannose-capped lipoarabinomannan of Bacillus Calmette-Guerin enhances immunoprotective effect against tuberculosis. J. Am. Chem. Soc. *138*, 11680–11689.

Taitano, S.H., van der Vlugt, L.E.P.M., Shea, M.M., Yang, J., Lukacs, N.W., and Lundy, S.K. (2018). Differential influence on regulatory B cells by th2 cytokines affects protection in allergic airway disease. J. Immunol. *201*, 1865–1874.

Upton, A.M., Cho, S., Yang, T.J., Kim, Y., Wang, Y., Lu, Y., Wang, B., Xu, J., Mdluli, K., Ma, Z., and Franzblau, S.G. (2015). In vitro and in vivo activities of the nitroimidazole TBA-354 against *Mycobacterium tuberculosis*. Antimicrob. Agents Chemother. *59*, 136–144.

Vergne, I., Gilleron, M., and Nigou, J. (2014). Manipulation of the endocytic pathway and phagocyte functions by *Mycobacterium tuberculosis* lipoarabinomannan. Front. Cell. Infect. Microbiol. *4*, 187.

Wagner, E.F., Hleb, M., Hanna, N., and Sharma, S. (1998). A pivotal role of cyclin D3 and cyclin-dependent kinase inhibitor p27 in the regulation of IL-2-, IL-4-, or IL-10-mediated human B cell proliferation. J. Immunol. *161*, 1123–1131.

Walsh, N.C., Waters, L.R., Fowler, J.A., Lin, M., Cunningham, C.R., Brooks, D.G., Rehg, J.E., Morse, H.C., 3rd, and Teitell, M.A. (2015). Teitell, LKB1 inhibition of NF-kappaB in B cells prevents T follicular helper cell differentiation and germinal center formation. EMBO Rep. *16*, 753–768.

Wang, J., Li, B.X., Ge, P.P., Li, J., Wang, Q., Gao, G.F., Qiu, X.B., and Liu, C.H. (2015). *Mycobacterium tuberculosis* suppresses innate immunity by coopting the host ubiquitin system. Nat. Immunol. *16*, 237–245.

Wang, J.Y., Chang, H.C., Liu, J.L., Shu, C.C., Lee, C.H., Wang, J.T., and Lee, L.N. (2012). Expression of toll-like receptor 2 and plasma level of interleukin-10 are associated with outcome in tuberculosis. Eur. J. Clin. Microbiol. Infect. Dis. *31*, 2327–2333.

Worakitkanchanakul, W., Imura, T., Fukuoka, T., Morita, T., Sakai, H., Abe, M., Rujiravanit, R., Chavadej, S., Minamikawa, H., and Kitamoto, D. (2008). Aqueous-phase behavior and vesicle formation of natural glycolipid biosurfactant, mannosylerythritol lipid-B. Colloids Surf. B Biointerfaces *65*, 106–112.

Yanaba, K., Bouaziz, J.D., Haas, K.M., Poe, J.C., Fujimoto, M., and Tedder, T.F. (2008). A regulatory B cell subset with a unique CD1dhiCD5+ phenotype controls T cell-dependent inflammatory responses. Immunity *28*, 639–650.

Yang, M., Rui, K., Wang, S., and Lu, L. (2013). Regulatory B cells in autoimmune diseases. Cell. Mol. Immunol. *10*, 122–132.

Yonekawa, A., Saijo, S., Hoshino, Y., Miyake, Y., Ishikawa, E., Suzukawa, M., Inoue, H., Tanaka, M., Yoneyama, M., Oh-Hora, M., et al. (2014). Dectin-2 is a direct receptor for mannose-capped lipoarabinomannan of mycobacteria. Immunity *41*, 402–413.

Zajonc, D.M., Ainge, G.D., Painter, G.F., Severn, W.B., and Wilson, I.A. (2006). Structural characterization of mycobacterial phosphatidylinositol mannoside binding to mouse CD1d. J. Immunol. *177*, 4577–4583.

ISCI, Volume *11*

Supplemental Information

Mycobacterium tuberculosis Mannose-Capped Lipoarabinomannan Induces IL-10-Producing B Cells and Hinders $CD4^+$Th1 Immunity

Chunhui Yuan, Zi-Lu Qu, Xiao-Lei Tang, Qi Liu, Wei Luo, Chun Huang, Qin Pan, and Xiao-Lian Zhang

Supplemental Information

Figure S1

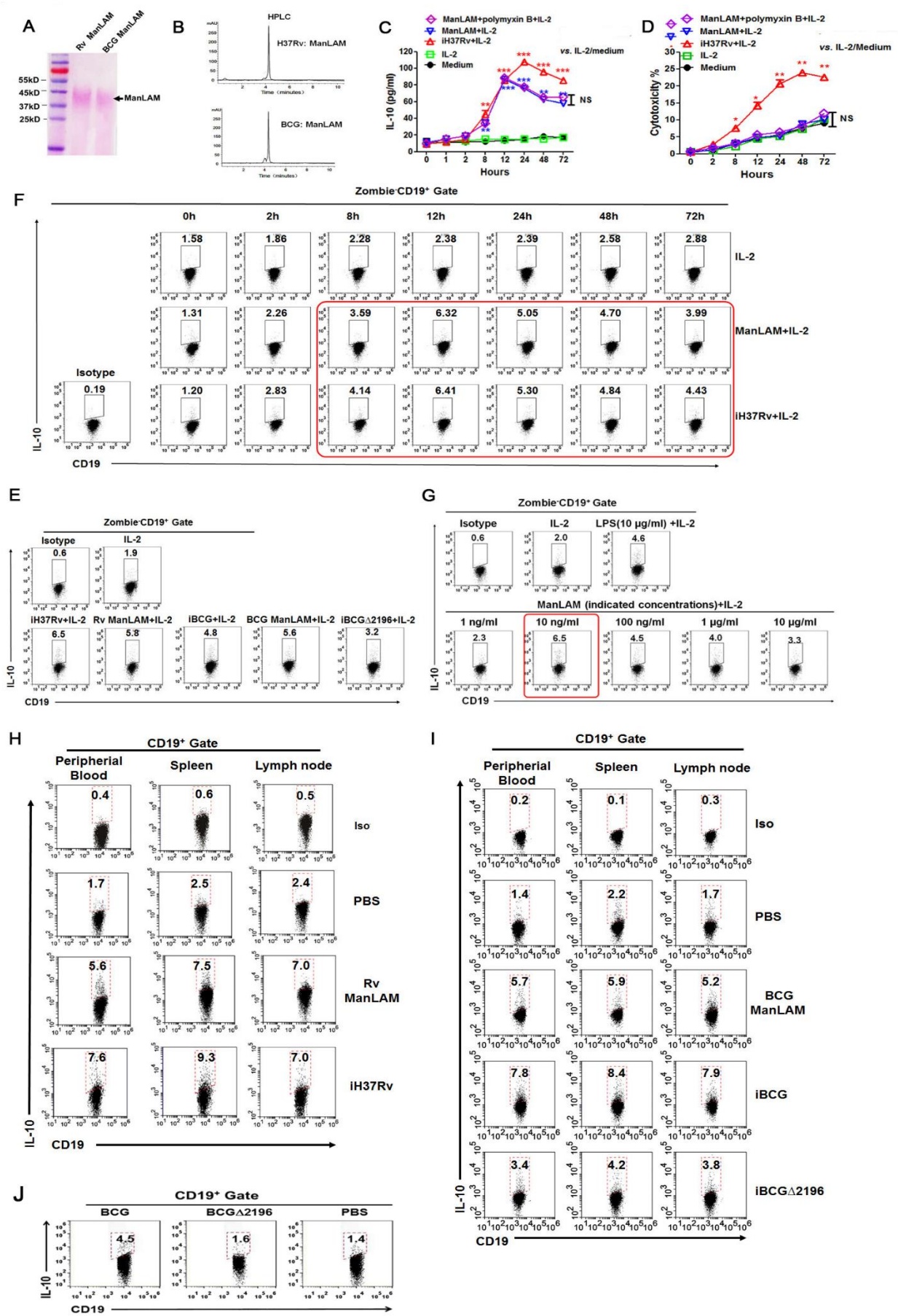
A
Rv ManLAM
BCG ManLAM
55kD
45kD
37kD
25kD
ManLAM
B
HPLC
H37Rv: ManLAM
BCG: ManLAM
Time (minutes)
C
ManLAM+polymyxin B+IL-2
ManLAM+IL-2
iH37Rv+IL-2
IL-2
Medium
vs. IL-2/medium
IL-10 (pg/ml)
NS
Hours
D
ManLAM+polymyxin B+IL-2
ManLAM+IL-2
iH37Rv+IL-2
IL-2
Medium
vs. IL-2/Medium
Cytotoxicity %
NS
Hours
F
Zombie-CD19+ Gate
0h
2h
8h
12h
24h
48h
72h
IL-2
ManLAM+IL-2
iH37Rv+IL-2
Isotype
IL-10
CD19
E
Zombie-CD19+ Gate
Isotype
IL-2
iH37Rv+IL-2
Rv ManLAM+IL-2
iBCG+IL-2
BCG ManLAM+IL-2
iBCGΔ2196+IL-2
IL-10
CD19
G
Zombie-CD19+ Gate
Isotype
IL-2
LPS(10 μg/ml) +IL-2
ManLAM (indicated concentrations)+IL-2
1 ng/ml
10 ng/ml
100 ng/ml
1 μg/ml
10 μg/ml
IL-10
CD19
H
CD19+ Gate
Peripherial Blood
Spleen
Lymph node
Iso
PBS
Rv ManLAM
iH37Rv
IL-10
CD19
I
CD19+ Gate
Peripherial Blood
Spleen
Lymph node
Iso
PBS
BCG ManLAM
iBCG
iBCGΔ2196
IL-10
CD19
J
CD19+ Gate
BCG
BCGΔ2196
PBS
IL-10
CD19

Figure S1. [Murine B cells produce IL-10 upon stimulation with *M. tb*/ ManLAM], Related to Figure 2.

(A) ManLAM was detected by sodium dodecyl sulfate–polyacrylamide gel electrophoresis (visualized by glycogen staining).

(B) The final preparation of ManLAM from *M. tb* H37Rv or BCG determined by high-performance liquid chromatography (HPLC).

(C) and (D) Time course of IL-10 production in ManLAM-treated B cells and ManLAM cytotoxicity against B cells. Splenic B cells were stimulated *in vitro* with iH37Rv (MOI, 1:2), Rv ManLAM (10 ng/ml) or polymyxin B-treated ManLAM for the indicated time periods (0-72 h). (C) IL-10 production in the cell culture supernatant was detected by ELISA. (D) Cytotoxicity was determined and ManLAM showed low toxicity at a concentration of 10 ng/ml.

(E) B cells produced IL-10 upon stimulation with iH37Rv/iBCG/iBCGΔ2196/ManLAM *in vitro*. Splenic B cells were stimulated with iH37Rv, Rv ManLAM, iBCG (MOI, 1:2), iBCGΔ2196 (MOI, 1:2) or BCG ManLAM (10 ng/ml) for 12 h. B10 cells were detected by FCM. Representative dot plots.

(F) Time course of IL-10 production in ManLAM-treated B cells. B cells were stimulated with iH37Rv/Rv ManLAM (10 ng/ml) for the indicated time periods (0-72 h). B10 cells were detected by FCM. Representative dot plots.

(G) B cells produced IL-10 upon stimulation with various concentrations of Rv ManLAM *in vitro*. Representative dot plots.

(H) and (I) B cells produced IL-10 upon stimulation with iH37Rv/iBCG/iBCGΔ2196/ManLAM *in vivo*. Mice were injected (*i. p.*) with iH37Rv/iBCG/iBCGΔ2196 (10^8 CFU/100 μl/mouse) or ManLAM (100 ng/100 μl/mouse) on day 1 and day 7. After 12 h of the 2nd injection, B10 cells from peripheral

blood, spleen and inguinal lymph nodes were analyzed by FCM. Representative dot plots.

(J) Mice were infected (*i. v.*) with live BCG/BCGΔ2196 (6 mice each group). splenocytes were collected at day 20 post-infection and B10 cells were determined by FCM. Representative dot plots.

C-G, B cells were cultured in medium containing IL-2. Data are represented as mean ± SD. ***$p < 0.001$; **$p < 0.01$; *$p < 0.05$; NS, not significant.

Figure S2

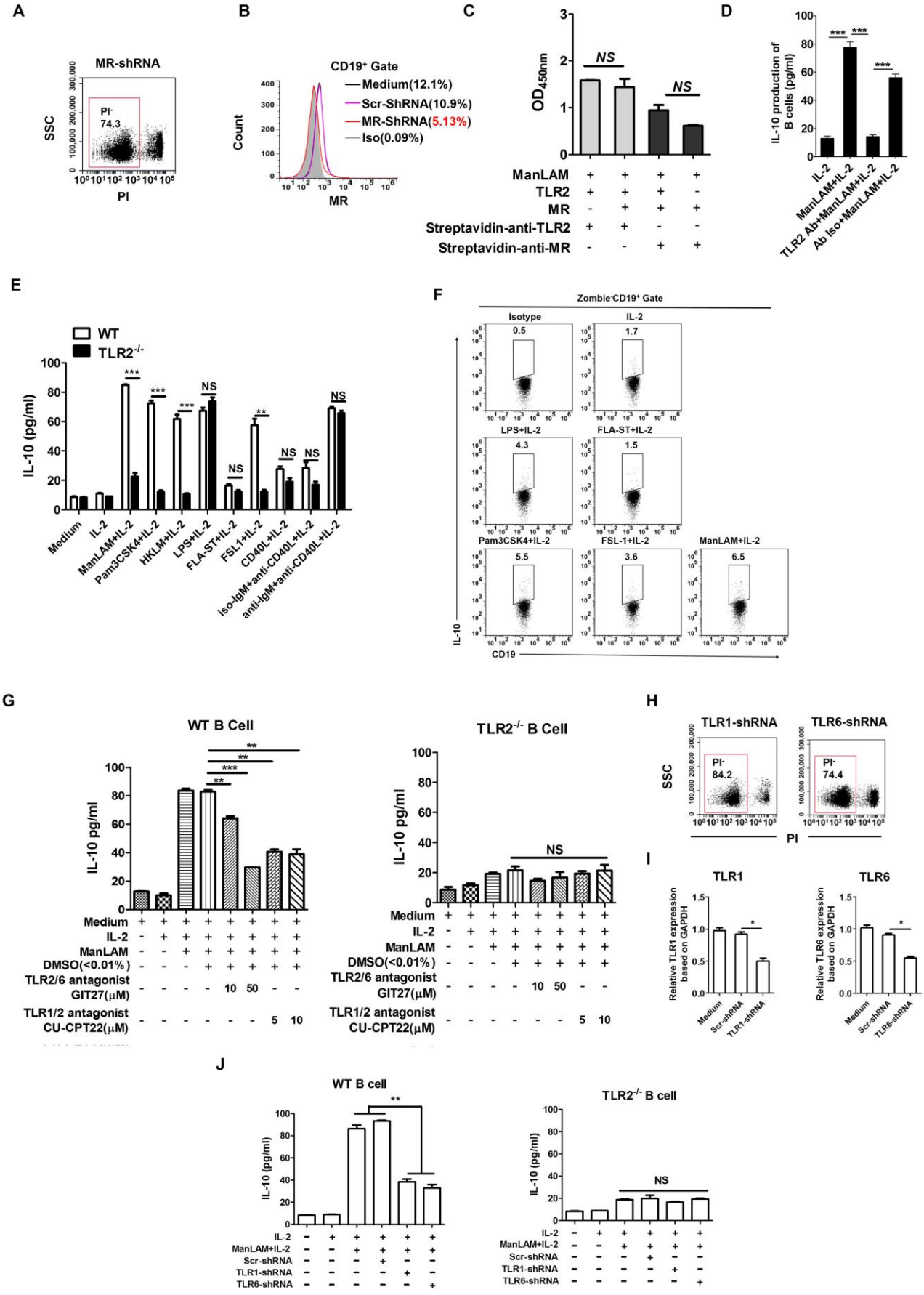
A
MR-shRNA
PI-
74.3
SSC
PI
B
CD19+ Gate
Medium(12.1%)
Scr-ShRNA(10.9%)
MR-ShRNA(5.13%)
Iso(0.09%)
Count
MR
C
OD450nm
NS
NS
ManLAM
TLR2
MR
Streptavidin-anti-TLR2
Streptavidin-anti-MR
D
IL-10 production of B cells (pg/ml)
IL-2
ManLAM+IL-2
TLR2 Ab+ManLAM+IL-2
Ab Iso+ManLAM+IL-2
E
WT
TLR2-/-
IL-10 (pg/ml)
Medium
IL-2
ManLAM+IL-2
Pam3CSK4+IL-2
HKLM+IL-2
LPS+IL-2
FLA-ST+IL-2
FSL1+IL-2
CD40L+IL-2
iso-IgM+anti-CD40L+IL-2
anti-IgM+anti-CD40L+IL-2
F
Zombie-CD19+ Gate
Isotype
IL-2
LPS+IL-2
FLA-ST+IL-2
Pam3CSK4+IL-2
FSL-1+IL-2
ManLAM+IL-2
IL-10
CD19
G
WT B Cell
TLR2-/- B Cell
IL-10 pg/ml
Medium
IL-2
ManLAM
DMSO(<0.01%)
TLR2/6 antagonist GIT27(μM)
TLR1/2 antagonist CU-CPT22(μM)
H
TLR1-shRNA
TLR6-shRNA
PI-
84.2
74.4
SSC
PI
I
TLR1
TLR6
Relative TLR1 expression based on GAPDH
Relative TLR6 expression based on GAPDH
Medium
Scr-shRNA
TLR1-shRNA
TLR6-shRNA
J
WT B cell
TLR2-/- B cell
IL-10 (pg/ml)
IL-2
ManLAM+IL-2
Scr-shRNA
TLR1-shRNA
TLR6-shRNA

Figure S2. [ManLAM binding to TLR2 stimulates IL-10 production by B cells], Related to Figure 3.

(A) Cell viability after 36 h of nucleofection with MR-shRNA was determined by PI staining. Cell viability was expressed as the percentage of PI^- cells.

(B) WT B cells were transfected with MR-shRNA or scramble shRNA. After 48 h, the MR expression was determined by FCM.

(C) Identified the binding sites of ManLAM for MR and TLR2 are different by ELISA.

(D) Anti-TLR2 antibody inhibited IL-10 production by B cells in response to Rv ManLAM stimulation. B cells were stimulated with ManLAM (10 ng/ml) in the presence of anti-TLR2 antibody (5 μg/ml) for 12 h. IL-10 production in the cell supernatant was determined by the CBA assay.

(E) $TLR2^{-/-}$ B cells were actually capable of producing IL-10 at similar levels to WT B cells. B cells were treated with ManLAM, TLR agonists or anti-IgM+CD40L for 12 h. IL-10 production in the culture supernatant was determined by ELISA.

(F) B10 levels were increased in the ManLAM, TLR1/2 agonist, TLR6/2 agonist and TLR4 agonist groups. B cells were stimulated with ManLAM or the indicated TLR agonists for 12 h. B10 levels were determined by FCM.

(G) B cells were pre-treated with TLR1 antagonist GIT-27 or with TLR6 antagonist CU-CPT22 before stimulation with ManLAM. IL-10 production by WT/TLR-$2^{-/-}$ B cells was determined by ELISA.

(H) Cell viability after 36 h of nucleofection with TLR1/TLR2-shRNA was determined by PI staining. Cell viability was expressed as the percentage of PI^- cells.

(I) WT B cells were transfected with TLR1-shRNA, TLR6-shRNA or scramble shRNA. After 24 h, mRNA expression levels of TLR1 or TLR6 were determined by qRT-PCR.

(J) IL-10 production by TLR1/TLR6-silenced and ManLAM-treated WT/TLR-$2^{-/-}$ B cells was determined by ELISA. D-G and J, B cells were cultured in medium containing IL-2. The data in C-E, G and I-J were shown as means ± SD. ***$p < 0.001$; **$p < 0.01$; *$p < 0.05$; NS, not significant.

Figure S3

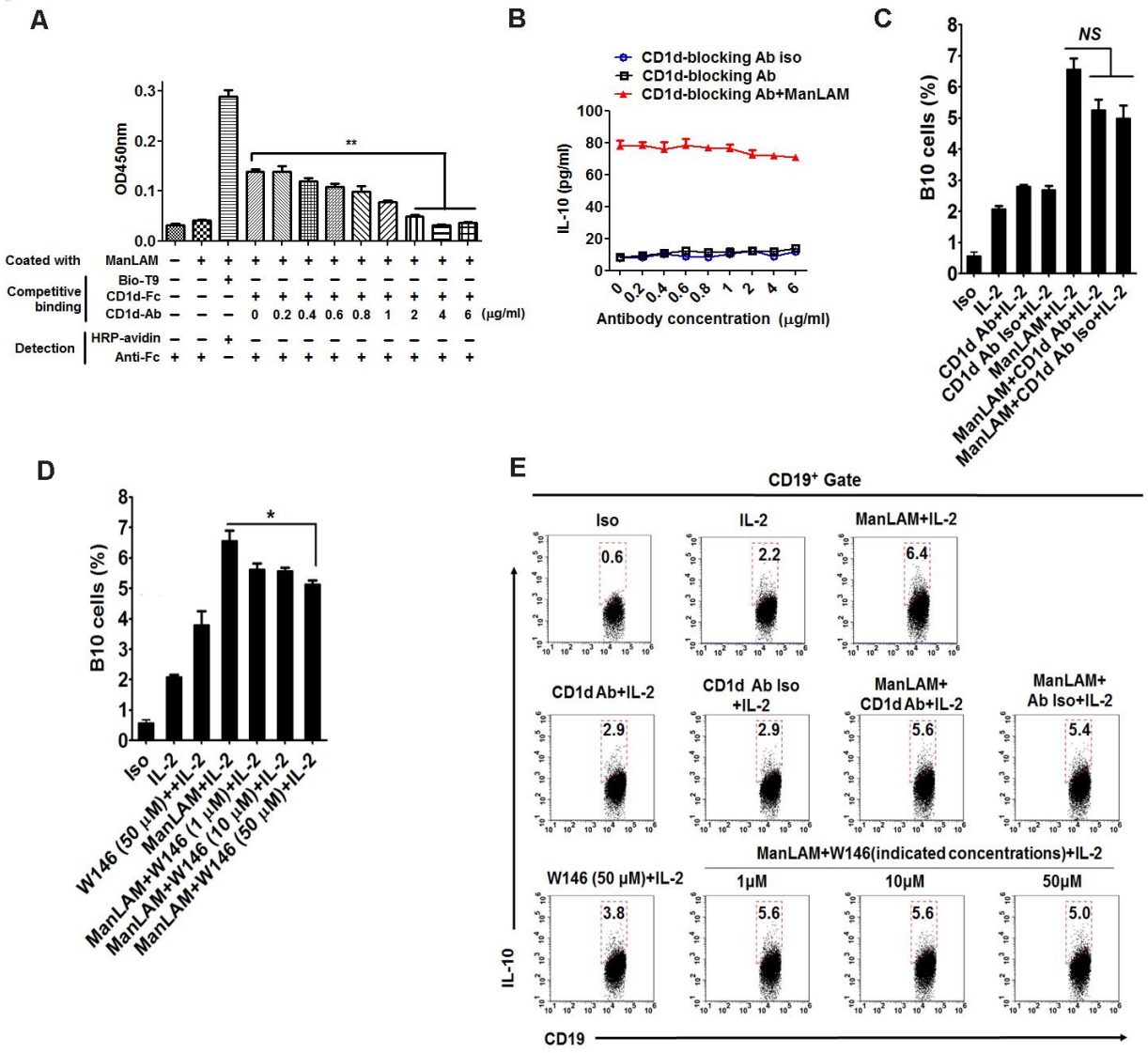

Figure S3. [IL-10 production by ManLAM-treated B cells was not mainly *via* CD1d and S1P$_1$], Related to Figure 3.

(A) Anti-CD1d antibody inhibited the binding of ManLAM to CD1d. The microplate was coated with ManLAM (10 ng/ml). CD1d-Fc protein (5 μg/ml) was added to the microplate in the presence of various concentrations of anti-CD1d antibody (0-6 μg/ml). After washing, the binding of ManLAM to CD1d was determined. In the positive control group, ManLAM was coated and the biotin-labeled ssDNA aptamer T9 was used to detect ManLAM.

(B) IL-10 production by ManLAM-treated B cells in the presence of anti-CD1d antibody was determined by ELISA.

(C)-(E) B10 cells were determined by FCM. B cells were pretreated with anti-CD1d antibody (5 μg/ml), Ab rat IgG2b κ Iso (5 μg/ml) and various concentrations of W146 ($S1P_1$ inhibitor) for 1 h, respectively. The cells were then stimulated with Rv ManLAM (10 ng/ml) for 12 h. C and D, pooled data. E, Representative dot plots. B-E, B cells were cultured in medium containing IL-2. The data in B-D were shown as means ± SD. **$p < 0.01$; *$p < 0.05$; NS, not significant.

Figure S4

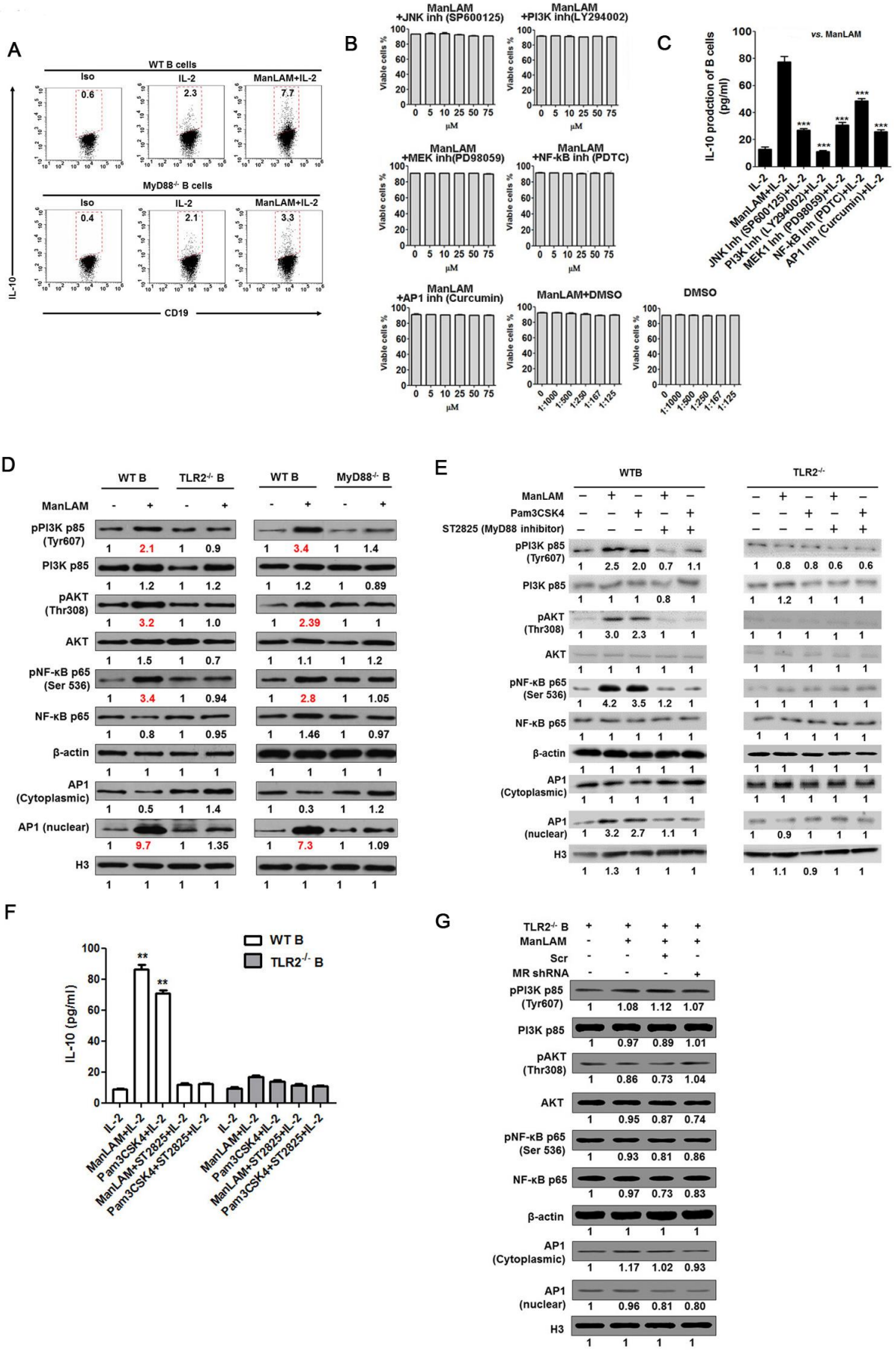
A
WT B cells
Iso
IL-2
ManLAM+IL-2
0.6
2.3
7.7
MyD88-/- B cells
0.4
2.1
3.3
IL-10
CD19
B
ManLAM +JNK inh (SP600125)
ManLAM +PI3K inh(LY294002)
ManLAM +MEK inh(PD98059)
ManLAM +NF-kB inh (PDTC)
ManLAM +AP1 inh (Curcumin)
ManLAM+DMSO
DMSO
Viable cells %
μM
C
IL-10 prodction of B cells (pg/ml)
vs. ManLAM
IL-2
ManLAM+IL-2
JNK Inh (SP600125)+IL-2
PI3K Inh (LY294002)+IL-2
MEK1 Inh (PD98059)+IL-2
NF-kB Inh (PDTC)+IL-2
AP1 Inh (Curcumin)+IL-2
D
WT B
TLR2-/- B
MyD88-/- B
ManLAM
pPI3K p85 (Tyr607)
PI3K p85
pAKT (Thr308)
AKT
pNF-κB p65 (Ser 536)
NF-κB p65
β-actin
AP1 (Cytoplasmic)
AP1 (nuclear)
H3
E
WTB
TLR2-/-
ManLAM
Pam3CSK4
ST2825 (MyD88 inhibitor)
F
WT B
TLR2-/- B
IL-10 (pg/ml)
IL-2
ManLAM+IL-2
Pam3CSK4+IL-2
ManLAM+ST2825+IL-2
Pam3CSK4+ST2825+IL-2
G
TLR2-/- B
ManLAM
Scr
MR shRNA

Figure S4. [IL-10 production by ManAM-treated B cells requires MyD88/PI3K/AKT/Ap-1 and NF-κB signaling pathways], Related to Figure 4.

(A) The B10 cells were analyzed by FCM. WT and MyD88$^{-/-}$ B cells were stimulated with Rv ManLAM (10 ng/ml) for 12 h. Representative dot plots.

(B) Cell viability. B cells were pretreated with the indicated inhibitors at various concentrations (0-75 μM) for 1 h. Cell viability at the end of culture for each inhibitor was determined by FCM with PI staining. The viability of the cells for each inhibitor was more than 90 %.

(C) IL-10 production of ManLAM-treated B cells was inhibited by AP1 and NF-κB inhibitors. B cells were pre-treated with the indicated inhibitors for 1 h and stimulated with ManLAM for 12 h. IL-10 in culture supernatant was analyzed by CBA kit.

(D) PI3K, AKT, NF-κB and AP1 expression and activation were determined in WT B cells and TLR2$^{-/-}$ B cells (or MyD88$^{-/-}$ B cells) upon stimulation with ManLAM for 1 h by immunoblotting. Representative blots.

(E) Immunoblotting analysis of PI3K, AKT, NF-κB and AP1 expression and activation in WT B cells and TLR2$^{-/-}$ B cells upon ManLAM/ Pam3CSK4 stimulation with or without MyD88 inhibitor.

(F) IL-10 production in WT/TLR2$^{-/-}$ B cells upon stimulation with ManLAM/Pam3CSK4 for 12 h with or without MyD88 inhibitor was determined by ELISA.

(G) PI3K, AKT, AP1 and NF-κB expression and activation in MR-silenced TLR2$^{-/-}$ B cells upon stimulation with ManLAM for 1 h were determined by immunoblotting. A-G, B cells were cultured in medium containing IL-2. Data in B, C and F were shown as means ± SD. ***$p < 0.001$; **$p < 0.01$.

Figure S5

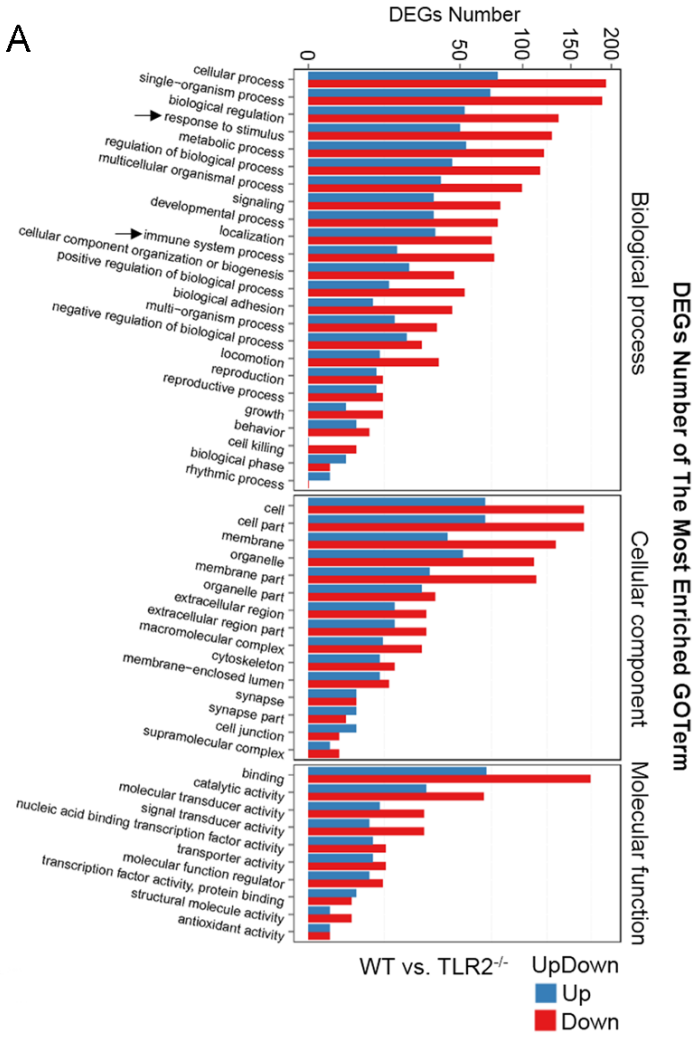
A
DEGs Number
0
50
100
150
200
cellular process
single−organism process
biological regulation
response to stimulus
metabolic process
regulation of biological process
multicellular organismal process
signaling
developmental process
localization
immune system process
cellular component organization or biogenesis
positive regulation of biological process
biological adhesion
multi−organism process
negative regulation of biological process
locomotion
reproduction
reproductive process
growth
behavior
cell killing
biological phase
rhythmic process
Biological process
cell
cell part
membrane
organelle
membrane part
organelle part
extracellular region
extracellular region part
macromolecular complex
cytoskeleton
membrane−enclosed lumen
synapse
synapse part
cell junction
supramolecular complex
Cellular component
binding
catalytic activity
molecular transducer activity
signal transducer activity
nucleic acid binding transcription factor activity
transporter activity
molecular function regulator
transcription factor activity, protein binding
structural molecule activity
antioxidant activity
Molecular function
DEGs Number of The Most Enriched GOTerm
WT vs. TLR2-/-
UpDown
Up
Down

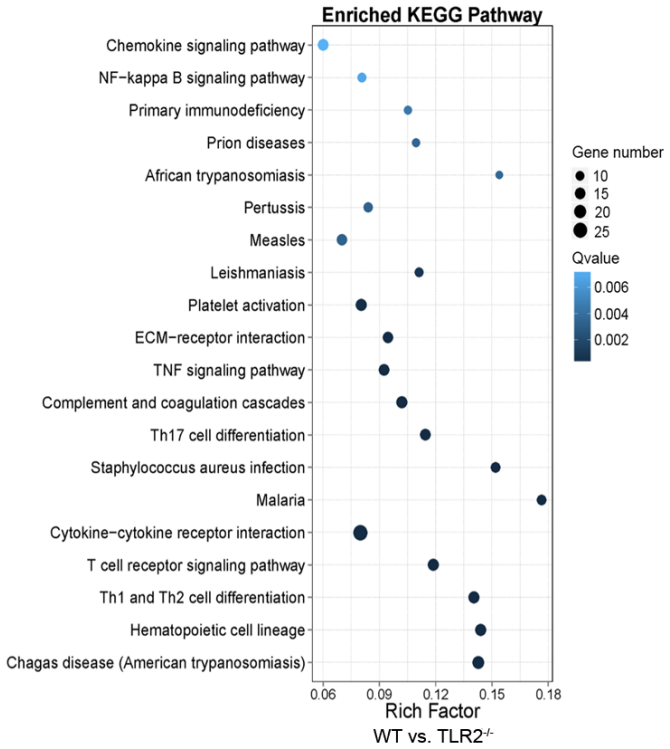
B
Enriched KEGG Pathway
Chemokine signaling pathway
NF−kappa B signaling pathway
Primary immunodeficiency
Prion diseases
African trypanosomiasis
Pertussis
Measles
Leishmaniasis
Platelet activation
ECM−receptor interaction
TNF signaling pathway
Complement and coagulation cascades
Th17 cell differentiation
Staphylococcus aureus infection
Malaria
Cytokine−cytokine receptor interaction
T cell receptor signaling pathway
Th1 and Th2 cell differentiation
Hematopoietic cell lineage
Chagas disease (American trypanosomiasis)
0.06
0.09
0.12
0.15
0.18
Rich Factor
WT vs. TLR2-/-
Gene number
10
15
20
25
Qvalue
0.006
0.004
0.002

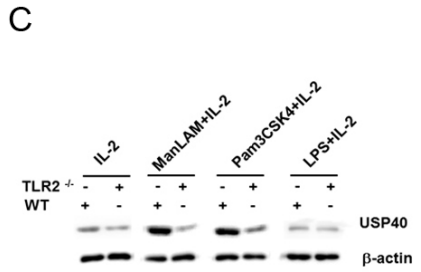
C
IL-2
ManLAM+IL-2
Pam3CSK4+IL-2
LPS+IL-2
TLR2 -/-
WT
USP40
β-actin

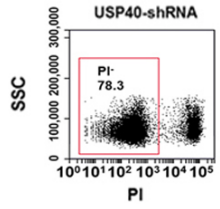
D
USP40-shRNA
PI-
78.3
SSC
PI

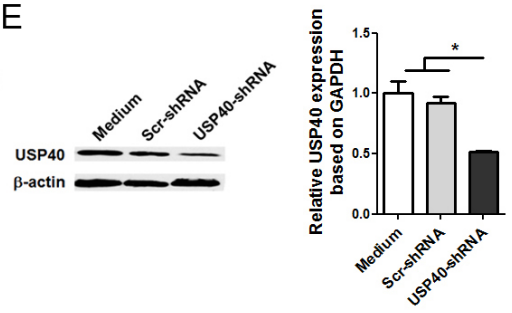
E
Medium
Scr-shRNA
USP40-shRNA
USP40
β-actin
Relative USP40 expression based on GAPDH
1.5
1.0
0.5
0.0
*
Medium
Scr-shRNA
USP40-shRNA

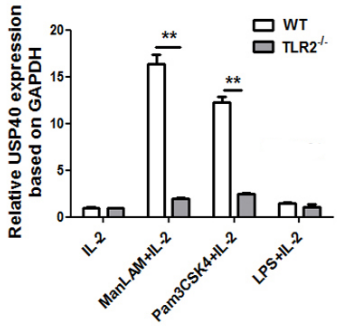
Relative USP40 expression based on GAPDH
20
15
10
5
0
**
**
WT
TLR2-/-
IL-2
ManLAM+IL-2
Pam3CSK4+IL-2
LPS+IL-2

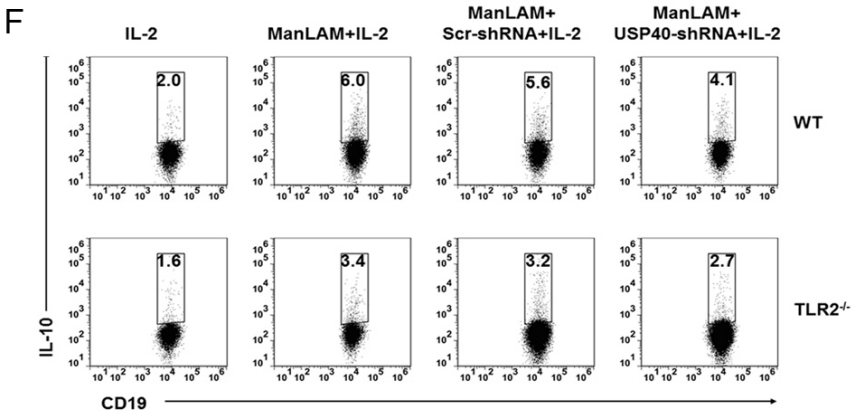
F
IL-2
ManLAM+IL-2
ManLAM+ Scr-shRNA+IL-2
ManLAM+ USP40-shRNA+IL-2
2.0
6.0
5.6
4.1
WT
1.6
3.4
3.2
2.7
TLR2-/-
IL-10
CD19

Figure S5. [ManAM induces B10 cells *via* TLR2 and USP40], Related to Figure 5.

(A) and (B) GO and Kyoto Encyclopedia of Genes and Genomes (KEGG) enrichment of differentially expressed genes in WT *vs*. TLR2$^{-/-}$. (A) GO categories enrichment (FDR <=0.01). (B) KEGG pathway enrichment (FDR <=0.01).

(C) USP40 mRNA and protein expression. WT/TLR2$^{-/-}$ B cells were stimulated with Rv ManLAM (10 ng/ml) , TLR2 agonist (Pam3CSK4, 300 ng/ml) or TLR4 agonist (LPS, 10 μg/ml) for 12 h. Upper panel, protein expression of USP40 was analyzed by immunoblotting, using β-actin as an internal control. Lower panel, qRT-PCR was used to detect the mRNA expression of USP40, and GAPDH was used as an internal control.

(D) Cell viability after 36 h of nucleofection with USP40-shRNA was determined by FCM with PI staining. Cell viability was expressed as the percentage of PI^{-} cells.

(E) WT B cells were transfected with Scr or USP40-shRNA. After 24 h, the mRNA expression of USP40 was determined by qRT-PCR (right panel), and after 48 h, the USP40 expression was determined by immunoblotting (left panel).

(F) ManAM induced B10 cells *via* TLR2 and USP40. WT B and TLR2$^{-/-}$ cells were transfected with USP40 shRNA. After 48 h, WT and TLR2$^{-/-}$ B cells were stimulated with Rv ManLAM for 12 h. B10 cells were detected by FCM. Representative dot plots. C and F, B cells were cultured in medium containing IL-2. Data in C and E were shown as means ± SD. **p < 0.01; *p < 0.05; NS, not significant.

Figure S6

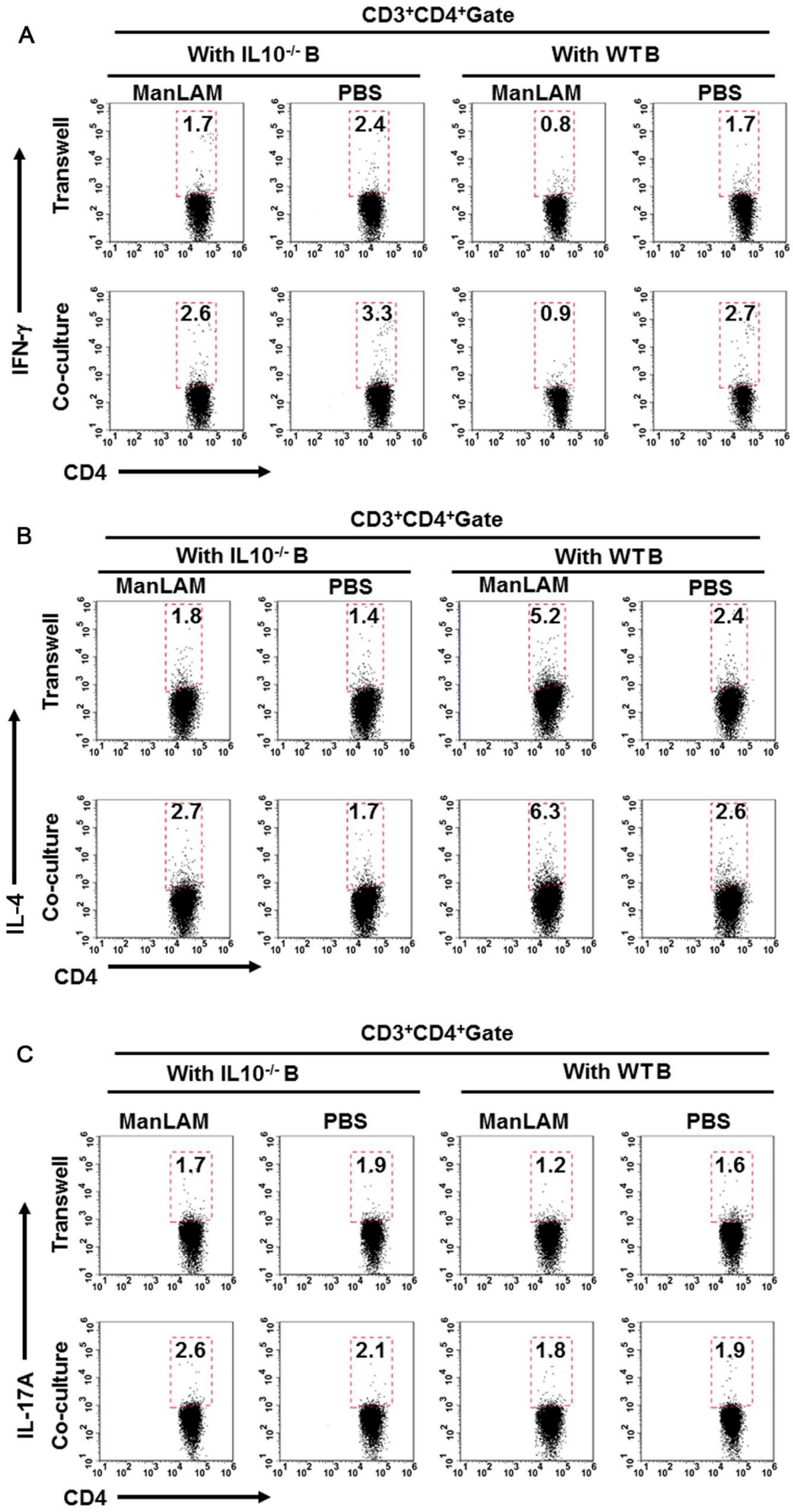
A
CD3+CD4+Gate
With IL10-/- B
With WTB
ManLAM
PBS
ManLAM
PBS
Transwell
1.7
2.4
0.8
1.7
Co-culture
2.6
3.3
0.9
2.7
IFN-γ
CD4
B
CD3+CD4+Gate
With IL10-/- B
With WTB
ManLAM
PBS
ManLAM
PBS
Transwell
1.8
1.4
5.2
2.4
Co-culture
2.7
1.7
6.3
2.6
IL-4
CD4
C
CD3+CD4+Gate
With IL10-/- B
With WTB
ManLAM
PBS
ManLAM
PBS
Transwell
1.7
1.9
1.2
1.6
Co-culture
2.6
2.1
1.8
1.9
IL-17A
CD4

Figure S6. [ManLAM-induced B10 cells inhibit Th1 polarization, promote Th2 polarization and have no effects on Th17 *in vitro*], Related to Figure 6. Splenic B cells were isolated from WT/IL-$10^{-/-}$ mice and stimulated with Rv ManLAM (10 ng/ml) in the presence of IL-2 (30 U/ml) for 12 h. Then ManLAM was removed by washing the cells. $CD4^+$ T cells were stimulated by plate-coated anti-CD3 antibody (5 μg/ml) and soluble anti-CD28 antibody (2 μg/ml) in the presence of the ManLAM-treated B cells for 72 h. In the transwell groups, T and B cells was separated by the microporous membrane and did not directly interact with each other. In the co-culture groups, T cells and B cells were mixed together and cultured. IFN-γ, IL-4 and IL-17A productions by $CD4^+$ T cells were analyzed by FCM. Representative dot plots of (A) IFN-γ, (B) IL-4 and (C) IL-17A production by $CD4^+$ T cells.

Figure S7

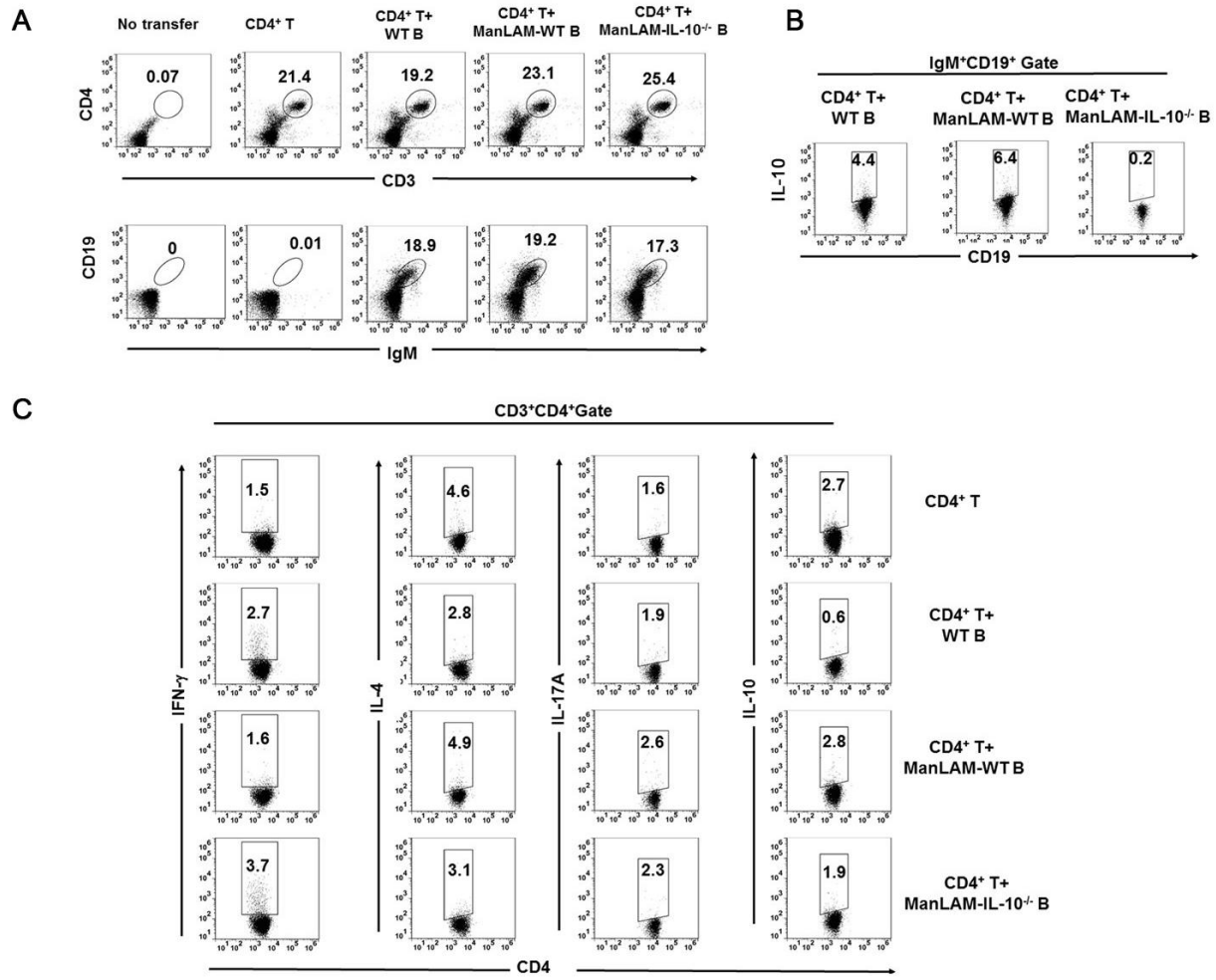

Figure S7. [ManLAM-induced IL-10 production by B cells increases susceptibility to BCG infection in mice], Related to Figure 8. Mice were adoptively transferred with ManLAM-treated WT/IL-$10^{-/-}$ B cells, and the mice were intravenously (*i. v.*) infected with BCG. (A) After 20 days of infection, adoptively transferred $CD3^{+}CD4^{+}$ T cells and $IgM^{+}CD19^{+}$ B cells in the spleens were determined by FCM. (B) Splenic B10 cells and (C) cytokines produced by $CD4^{+}$ T cells were determined by FCM. Representative dot plots.

Figure S8

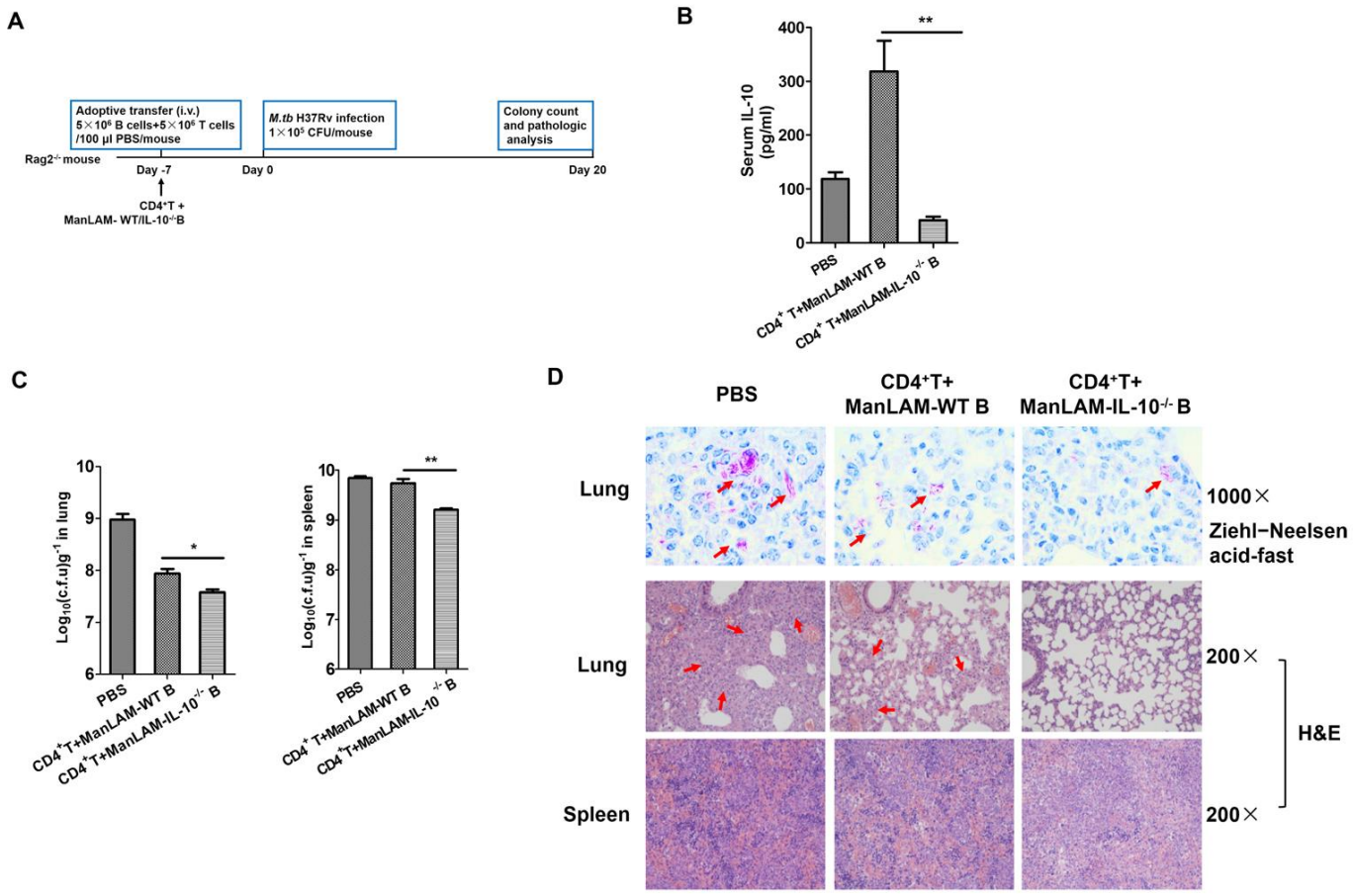

Figure S8. [ManLAM-induced IL-10 production by B cells increases susceptibility to virulent *M.tb* H37Rv infection in mice], Related to Figure 8. Mice were infected (*i. v.*) with *M.tb* H37Rv. (A) Schematic diagram. (B) After 20 days of infection, serum IL-10 were determined by ELISA. (C) *M.tb* H37Rv CFU assay in lungs and spleens. (D) Upper panel, lung tissue sections were analyzed with Ziehl–Neelsen acid-fast stain (1000 ×). The arrows represent the bacteria. Lower panel, lung and spleen tissue sections were stained with hematoxylin and eosin (H&E) and evaluated by light microscopy (200×). The arrows indicate the pulmonary lesions. Data in B and C were shown as means ± D. **p < 0.01; *p < 0.05.

Transparent Methods

Patient samples

Peripheral blood samples from a total of 30 patients with newly diagnosed active pulmonary tuberculosis and 30 healthy donors from Wuhan Medical Treatment Center (Wuhan, China) and Zhongnan Hospital of Wuhan University (Wuhan, China). Blood samples were collected from ATB patients before medical treatment. The diagnosis of active tuberculosis was based on positive cultures for *M.tb*. TB patients co-infected with HIV or other diseases were excluded from the study. PBMCs were obtained by Ficoll density gradient centrifugation (Axis-Shield, Oslo, Norway) and then red blood cells were removed by applying Red Blood Cell Lysis Buffer (Beyotime, Shanghai, China).

Bacteria, ManLAM preparation, plasmids and animals

M.tb H37Rv (American Type Culture Collection (ATCC) strain 93009), *M. bovis* BCG (Sun et al., 2016) (ATCC strain 35734) and BCGΔ2196 (Sun et al., 2016) were maintained on Lowenstein-Jensen (L-J) medium and harvested while in log phase growth. *M.tb* H37Rv and *M. bovis* BCG were inactivated at 65 ℃ for 2 h. ManLAM was extracted from delipidated cells of inactivated *M.tb* H37Rv/ *M. bovis* BCG, purified by HPLC (high performance liquid chromatography) and identified as described in our previous report (Pan et al., 2014; Sun et al., 2016).

The construction of BCGΔ2196 has been described in our previous study (Sun et al., 2016). We used a homologous recombination method to delete the BCG2196 gene in the BCG strain. The BCG2196 gene is a major gene encoding the enzyme responsible for the synthesis of ManLAM.

The plasmids encoding WT ubiquitin and ubiquitin mutants were kindly provided by Dr. Hong-Bing Shu and Dr. Yan-Yi Wang. For the ubiquitin mutant plasmids, the Lys48 (ubiquitin-K48) and Lys63 (ubiquitin-K63) were mutated into arginines in the ubiquitin mutant H-Ub (K48) and H-Ub (K63) respectively (Zhong et al., 2009).

IL10$^{-/-}$, TLR2$^{-/-}$ and MyD88$^{-/-}$ C57BL/6J mice were obtained from Nanjing Biomedical Institute of Nangjing University. Rag2$^{-/-}$ mice were kindly provided by Dr Youchun Wang (National Institutes for Food and Drug Control, Beijing, China). μMT mice were kindly provided by Dr. Hai Qi (University of Tsinghua, Beijing, China). WT C57BL/6J, TLR4$^{-/-}$ and WT C3H/He mice were purchased from the Animal Laboratory Center of Wuhan University, China. Mice were bred and maintained in the animal facilities of the Animal Laboratory Center of Wuhan University (Wuhan, China).

Construction of shRNA expression vectors and nucleofection

The pSilencer 1.0-U6 (Ambion Life Technologies, Carlsbad, CA, USA) was used as described in our previous work (Li et al., 2008). The pSilencer 1.0-U6 has the U6 promoter. The 21-mer short hairpin RNAs (shRNAs) against *Mus musculus* MR (GenBank accession no. NM_008625), TLR1 (GenBank accession no. NM_030682), TLR6 (GenBank accession no. NM_011604) and USP40 (GenBank accession no. NM_001198573) mRNAs were designed. According to the targeting sequences, two pairs of oligonucleotides coding for each shRNA were designed. MR-Pair1: 5'-GCGAGAGATTATGGAACAAAGTTCA-3' (forward), 5'-AGCTTCTTTGTTCCATAATCTCTCGCGGCC-3' (reverse); MR-Pair2: 5'-AGCTTCTTTGTTCCATAATCTCTCGCTTTTT-3' (forward); 5'-AATTAAAAAGCGAGAGATTATGGAACAAAGA-3' (reverse). TLR1-Pair1: 5'-GCATTTGGACCTCTCCTTTAATTCA-3' (forward), 5'-

AGCTTGAATTAAAGGAGAGGTCCAAATGCGGCC-3’ (reverse); TLR1-Pair2: 5’-AGCTTTTAAAGGAGAGGTCAAATGCTTTTT-3’ (forward); 5’-AATTAAAAAGCATTTGGACCTCTCCTTTAAA-3’ (reverse). TLR6-Pair1: 5’-GGGAGTTTCCACTTTGTTTGCTTCA-3’ (forward); 5’-AGCTTGAAGCAAACAAAGTGGAAACTCCCGGCC-3’ (reverse); TLR6-Pair2: 5’-AGCTTGCAAACAAAGTGGAAACTCCCTTTTT-3’ (forward); 5’-AATTAAAAAGGGAGTTTCCACTTTGTTTGCA-3’ (reverse). USP40-pair1: 5’-GAACAGCTGTTTGAGACCCATTGATTTCA-3’ (forward), 5’-AGCTTGAAATCAATGGGTCTCAAACAGCTGTTCGGCC-3’ (reverse); USP40-pair 2: 5’-AGCTTATCAATGGGTCTCAAACAGCTGTTCTTTTTT-3’ (forward), 5’-AATTAAAAAAGAACAGCTGTTTGAGACCCATTGATA-3’ (reverse). Scramble(Scr)-shRNA-Pair1: 5’-CTGACCGACTATCGAGCACAGTTCA-3’ (forward); 5’-AGCTTCTGTGCTCGATAGTCGGTCAGGGCC-3’ (reverse); Scr-shRNA-Pair2: 5’-AGCTTCTGTGCTCGATAGTCGGTCAGTTTTT-3’ (forward); 5’-AATTAAAAACTGACCGACTATCGAGCACAGA-3’ (reverse).

The pairs of oligonucleotides were synthesized, annealed and inserted into the pSilencer vector. The recombinant vectors were transformed into *E. coli* DH5α. Each shRNA sequence contained a 9-bp loop sequence that separated the two complementary domains. The sequences for the complete shRNA insert templates were as follows. MR-shRNA 5'-GCGAGAGATTATGGAACAAAGTTCAAGCTTCTTTGTTCCATAATCTCTCGCTTTTT-3’(sense); 5'-AATTAAAAAGCGAGAGATTATGGAACAAAGAAGCTTGAACTTTGTTCCATAATCTCTCGCGGCC-3’(antisense). TLR1-shRNA 5’-GCATTTGGACCTCTCCTTTAATTCAAGCTTTTAAAGGAGAGGTCCAAATGC

TTTTT-3’(sense); 5’-AATTAAAAAGCATTTGGACCTCTCCTTTAAAAGCTTGAATTAAAGGAGAGGTCCAAATGCGGCC-3’(antisense). TLR6-shRNA 5’-GGGAGTTTCCACTTTGTTTGCTTCAAGCTTGCAAACAAAGTGGAAACTCCCTTTTT-3’(sense); USP40-shRNA 5’-GAACAGCTGTTTGAGACCCATTGATTTCAAGCTTATCAATGGGTCTCAAACAGCTGTTCTTTTTT-3’(sense); 5'- 5’-AATTAAAAAAGAACAGCTGTTTGAGACCCATTGATAAGCTTGAAATCAATGGGTCTCAAACAGCTGTTCGGCC-3’(antisense). Scr-shRNA 5’-CTGACCGACTATCGAGCACAGTTCAAGCTTCTGTGCTCGATAGTCGGTCAGTTTTT-3’ (sense); 5’-AATTAAAAACTGACCGACTATCGAGCACAGAAGCTTCTGTGCTCGATAGTCGGTCAGGGCC-3’(antisense).

B cells were nucleofected with shRNA vectors by using the Nucleofector™ System (Lonza, Basel, Switzerland) according to the manufacturer's instructions. Briefly, 3×10^6 cells were transfected with 2 μg of plasmid DNA in 100 μl of P3 Primary Cell 4D-Nucleofector™ X Solution, and further cultured for 48 h. The transient transfection efficiency of the cells was measured by using green fluorescent protein (GFP) as a reporter molecule. The percentage of transfected cells was determined by using pEGFP-C1 plasmid, which encodes GFP, cotransfected with pSilence-1.0-shRNAs into B cells using Nucleofector™ System. The efficiency of positive transfected cells were 60~70%. We detected the viability of transected cells by FCM with propidium iodide (PI) staining.

Magnetic activated cell sorting (MACS)

B cells were purified and isolated from splenocytes of mice using CD19 positive Magnetic Activated Cell Sorting (#130-052-201, Miltenyi Biotec, Bergisch Gladbach, Germany). Briefly, mouse splenocytes were incubated with microbeads-conjugated monoclonal rat anti-mouse CD19 antibodies at 4 ℃ for 15 min. After immobilization of all these cells with a magnet, untouched $CD19^-$ cells were discharged. $CD19^+$ B cells were then flushed from the column. The EasySep™ Mouse $CD4^+$ T Cell Isolation Kit (#19852, Stemcell Technologies, Canada) was used to isolate $CD4^+$ T cells from splenocytes by negative selection. Unwanted cells are targeted for removal with biotinylated antibodies directed against non-$CD4^+$ T cells and streptavidin-coated magnetic particles. The labeled cells were separated using an EasySep™ magnet, and the desired $CD4^+$ T cells were poured off into a new tube. The purity of the B cells and $CD4^+$ T cells was > 95 % as determined by FCM.

Flow cytometry (FCM)

To detect human B10 cells during TB infection, the blood of TB patients was treated with RBC lysis buffer (Beyotime, Shanghai, China) to eliminate red cells. The samples were not stimulated *in vitro* before FCM analysis. The samples incubated with human Fc Receptor Blocking Solution (#422302, Biolegend), which composed anti-human CD16 (3G8), CD32 (FUN-2), and CD64 (10.1) antibodies, to block FcRs, followed by staining with FITC anti-CD19 (SJ25C1), APC anti-IL-10 (JES3-9D7) and APC Rat IgG1, κ Isotype Ctrl Antibody (RTK2071) antibodies for FCM analysis. The blood samples were collected from patients with active TB.

For live-dead discrimination, Zombie Aqua™ Fixable Viability Kit (Biolegend #423102) was used in the detection of intracellular cytokines. PI^- staining was used in

determination of cell viability after nucleofection. Cell viability was expressed as the percentage of PI^- cells.

For detection of surface molecules on B cells, FITC anti-MR (C068C2), PE anti-CD40 (3/23), PE anti-CD80 (16-10A1), PE anti-CD83 (Michel-19), APC anti-CD86 (GL-1), perCP/Cy5.5 anti-mouse I-Ab (AF6-120) and percp/cy5.5 anti-IgM (RMM-1) antibodies were used.

For murine B10 cell detection *in vitro*, purified B cells (2×10^6) were cultured in the medium containing IL-2 (30U/ml, #212-12, Peprotech, NJ). The B cells were stimulated with various concentrations of ManLAM (1 -10^4 ng/ml) for 12 h. In the LPS control group, B cells were stimulated with 10 μg/ml of LPS for 12 h. 6 h before harvesting the cells, brefeldin A (1000×) was added. The B cells were incubated with anti-mouse CD16/CD32 antibody (clone 93) to block FcRs and stained with APC/FITC anti-CD19 (6D5), APC anti-mouse CD1d (CD1.1， Ly-38), PerCP-Cy5.5 anti-CD5 (53-7.3) antibodies and then fixed and permeabilized with fixation/permeabilization buffer (Biolegend, CA, USA) according to the manufacturer's protocol. Permeabilized cells were stained with PE anti-IL-10 antibody (JES5-16E3) or isotype control PE Rat IgG2b, κ Isotype. In the *in vivo* experiments, splenocytes isolated from infected mice were cultured in medium containing IL-2 (30 U/ml) and Brefeldin A (5 μg/ml) for 6 h, then the $CD19^+$B cells were assessed for intracellular cytokine expression by FCM.

To assess the effects of various TLR ligands (InvivoGen, San Diego, USA) on B10 cell induction, the TLR1/2 agonist Pam3CSK4 (100 ng/ml), TLR4 agonist LPS (10 μg/ml), TLR5 agonist-FLA-ST (flagellin from *Salmonella typhimurium*, 10 μg/ml) and TLR2/6 agonist FSL-1 (synthetic diacylated lipoprotein, 1 μg/ml) were used. After stimulation with 12 h, the B10 cells were determined.

To assess the effects of ManLAM binding to CD1d/$S1P_1$ on B10 cell induction, the cells were pre-treated with different concentrations of W146 ($S1P_1$ inhibitor, Bristol, United Kingdom, Tocris Bioscience), anti-CD1d antibody (5 μg/ml, 1B1) and Ab rat IgG2b κ Iso (5 μg/ml, RTK4530) for 1 h prior to ManLAM stimulation. The B10 cells were determined by FCM.

To identify the $CD4^+$ T cell polarization, APC-anti-CD3 (17A2), FITC-anti-CD4 (GK1.5), PE-anti-IL-4 (11B11), PE-anti-IFN-γ (XMG1.2) and PerCP-Cy5.5 anti-IL-17A (TC11-18H10.1) antibodies were used for the detection of intracellular cytokine expression. All antibodies used in the FCM analysis were purchased from Biolegend (CA, USA) and eBiosience (Thermo Fisher Scientific MA, USA).

Transwell and co-culture assay

Six-well plates were coated with anti-CD3 mAb (5 μg/ml) overnight at 4 ℃. $CD4^+$ T cells were purified from splenocytes using mouse BD IMag™ anti-mouse CD4 particles (GK1.5, BD PharMingen, CA, USA) *via* negative selection. The purified $CD4^+$ T cells were seeded in 6-well plates or lower transwell chambers at a density of 2×10^6 in 2 ml/well in the presence of soluble anti-CD28 (2 μg/ml) mAb. The 2×10^6 ManLAM-treated (WT or $IL10^{-/-}$) B cells were directly co-cultured with purified $CD4^+$T cells, or the B cells were added to the upper transwell chambers (Millicell, 0.4 μm; Millipore). After 72 h, IFN-γ/IL-4/IL-17A production by $CD4^+$ T cells was assessed by FCM.

Enzyme-linked immunosorbent assay (ELISA)

For IL-10 detection, murine splenic $CD19^+$ B cells (1×10^6 cells/ml) were stimulated with ManLAM (10 ng/ml), LPS (10 μg/ml) or iH37Rv (MOI, 1:2) in medium

containing IL-2 for 12 h. IL-10 production in the culture supernatants was detected by using a sandwich ELISA (Dakewe Biotech Co., Ltd., China).

To determine the IC_{50} of inhibitors for IL-10 production by B cells, B cells were pre-treated with LY294002 (PI3K inhibitor), PD98059 (MEK1 inhibitor), SP600125 (JNK inhibitor), curcumin (AP1 inhibitor) or PDTC (NF-κB inhibitor) at the indicated concentrations for 1 h before stimulation with ManLAM (10ng/ml) for 12 h.

To further identify the roles of TLR2 heterodimers involved in ManLAM-triggering signal pathway, B cells were pre-treated with TLR1 antagonist CU-CPT22 (MERCK #614305, Darmstadt, Germany) for 2 h or with TLR6 antagonist GIT-27 (BOC Science #6501-72-0, Shirley, USA) for 30 min before stimulation with ManLAM (10ng/ml) for 12 h.

Competition assay

ELISA plates were coated with Rv ManLAM (1 μg/ml) overnight at 4 ˚C. After blocking with 200 μl of bovine serum albumin (2 %, V/V) at 37 ˚C for 1 h, both MR (400 nM) and TLR2 (400 nM) proteins were added and incubated with ManLAM at 37 ˚C for 2 h. In the control groups, either MR (400 nM) protein (#Q2HZ94, R&D Systems, MN, USA) or TLR2 (400 nM, #1530-TR-050, R&D Systems, MN, USA) alone was added onto the ManLAM-coated plate. After washing, streptavidin-anti-TLR2/MR antibodies were added to detect the binding of TLR2/MR to ManLAM.

To assess the inhibition of ManLAM-CD1d binding by anti-CD1d antibody, ManLAM was used to coat the microplates. Recombinant mouse CD1d-Fc chimera protein (0.5 μg/100 μl, #4884-CD-050, R&D Systems, MN, USA R&D) was added on the microplate in the presence of various concentrations of anti-mouse CD1d

monoclonal antibody (mAb, #140804, Biolegend, CA). After incubation for 2 h, unbound CD1d-Fc was removed by washing. HRP-goat-anti-mouse IgG was added to detect CD1d bound to ManLAM. In the positive control groups, ManLAM was coated on the microplates, and Bio-T9 aptamer (Tang et al., 2016) was used to detect ManLAM.

Enzyme-linked oligonucleotide assay (ELONA)

To measure serum ManLAM in TB patients, we used aptamer-based indirect ELONA (Tang et al., 2014). Mannose receptor was coated on the microplates, and then the serum samples were added on the microplates. After washing, the biotin-labeled ssDNA ManLAM aptamer T9 (Tang et al., 2016) was added to detect serum ManLAM and HRP-streptavidin conjugate was used for color development. The absorbance at 450 nm was determined.

Cytometric-Bead Array (CBA)

B cells were pre-treated with LY294002 (PI3K inhibitor, 20 μM), PD98059 (MEK1 inhibitor, 20 μM), SP600125 (JNK inhibitor, 50 μM), curcumin (AP1 inhibitor, 10 μM), PDTC (NF-κB inhibitor, 20 μM), TLR2 blocking antibody and TLR2 Ab IgG1 κ Iso for 1 h. After washing, the cells were stimulated with ManLAM (10 ng/ml) for 12 h. The concentrations of IL-10 in culture supernatant was determined using the BD™ Cytometric Bead Array (CBA) Mouse Th1/Th2/Th17 Cytokine Kit (#560485, BD PharMingen, CA, USA) according to the manufacturer's protocol. The kit contained the beads conjugated to an antibody against IL-10. A secondary antibody conjugated to the fluorescent dye PE was used for detection.

ManLAM-beads pull-down assay

Whole cell lysate (WCL) was extracted using a membrane protein extraction kit (Beyotime Biotechnology, China). Then, 2 mg epoxy of magnetic beads (BioCanal, China) was washed with PBS and ethanol (100 %). The beads were hydroxylated in 500 μl of 20 mM 4-hydroxybenzhydrazide at 37 ˚C for 10 h. The beads were separated from the supernatants using a magnetic separation device for 3 min and then washed three times with 100 % ethanol. The hydroxyl modified beads were stored in 100 % ethanol at 4 ˚C. Rv ManLAM extracted from *M. tb* H37Rv was dissolved in the coupling buffer (0.2 mM of sodium acetate buffer, pH 5.4). After washing the beads with 100 % ethanol three times, the beads were conjugated to 2 mg of Rv ManLAM in 500 μl coupling buffer. The ManLAM-conjugated beads were incubated to 2 mg of cell membrane proteins in 500 μl of binding buffer (20 mM of Tris-HCl, 0.15 M of NaCl, 10 mM of $CaCl_2$, 6 mM of $MnCl_2$, pH 7.2) for 2 h at 37 ˚C with gentle shaking. Unbound proteins were removed from the beads by washing five or six times with washing buffer (20 mM of Tris-HCl, 0.25 mM of Tween-20, pH 7.2). The ManLAM-binding proteins that were bound to the beads were detected by immunoblotting.

Immunoprecipitation and immunoblot analysis

To detect the polyubiquitination of NEMO, B cells were transfected with the indicated plasmids encoding NEMO, WT ubiquitin (H-Ub), ubiquitin mutant H-Ub (K48) and H-Ub (K63) (*54*) At 48 h after transfection, the B cells were stimulated with ManLAM (10 ng/ml) for 12 h. The supernatant of the cell lysates was subjected for immunoprecipitation with an antibody against NEMO and then analyzed by immunoblotting with anti-ubiquitin antibody.

To detect p-PI3K p85 (Tyr607), PI3K p85, p-AKT (Thr308), AKT, p-NF-κB p65 (Ser 536), NF-κB p65, AP-1, Histone H3 and β-actin expression in ManLAM-treated

B cells, ManLAM-treated B cells were lysed in RIPA Lysis Buffer (Beyotime, shanghai, China), or the cytoplasmic and nuclear fractions of the B cells were prepared using a nuclear and cytoplasmic protein extraction kit (Beyotime, shanghai, China). Lysates were separated on a 5 % to 10 % SDS-polyacrylamide gel, transferred onto polyvinylidene difluoride membranes (Millipore) and then probed with specific antibodies. Bound antibodies were detected with HRP-conjugated secondary antibodies and visualized by chemiluminescence (Pierce ECL Western Blotting Substrate). Semi-quantification was carried out by densitometry using the UVP bioimaging system (Upland, CA, USA).

Transcriptional changes in ManLAM-treated CD1d^{hi}CD5^{+} B cells

WT/TLR2$^{-/-}$ B cells were stimulated with Rv ManLAM (10 ng/ml) for 12 h, and then the CD1d^{hi}CD5^{+} B cells were sorted by FCM. Total RNA was extracted from the sorted cells. The RNA was quantified using a NanoDrop ND-2000 (Thermo Scientific) and the RNA integrity was assessed using the Agilent Bioanalyzer 2100 (Agilent Technologies, USA) and then subjected to transcriptome analysis (BGISEQ-500 RNA-Seq, BGI Genomics, BGI-SHENZHEN, China). Briefly, the RNA samples were first treated with DNase I to remove DNA contamination. The mRNA molecules were then purified from the total RNA using oligo (dT) magnetic beads, and mRNA molecules were fragmented into small pieces. First-strand cDNA was generated using random hexamer primed reverse transcription, which was followed by second-strand synthesis. Adaptors were ligated to cDNA fragments for further hybridization. Subsequently, size-selected, adaptor-ligated cDNA was amplified by PCR. The quality of purified PCR products was evaluated using the Agilent Bioanalyzer 2100 (Agilent Technologies,

USA). The 3 prepared libraries were sequenced on the BGISEQ-500 platform with 50-bp single-end reads (BGI, China; http://www.seq50.com/en/)

After filtering low-quality reads, clean reads were mapped to the reference genome and genes using HISAT and Bowtie2 tool. For gene expression analysis, the matched reads were calculated and then normalized to FPKM using RESM software. The significance of the differential expression of genes was defined by the bioinformatics service of BGI according to the combination of the absolute value of the log2-Ratio $\geq$ 1 and FDR $\leq$ 0.001. Genome Ontology pathway over-representation analysis was performed on protein-coding genes that were differentially expressed using the WebGestaltR package (Wang et al., 2017). ClusterProfiler R package were used for KEGG pathway enrichment analysis (Yu et al., 2012). MEV software was used for hierarchical cluster analysis of gene expression patterns.

Quantitative Reverse Transcription PCR (qRT-PCR)

The B cells were stimulated with ManLAM (10 ng/ml) for 12 h. Total RNA was extracted from the cells and qRT-PCR analysis was performed. All primers for target and reference genes were as follows: F 5'-GGGACTGACATTCACCCTGG-3' and R 5'-GCATCTTCAAGTGACCCGGA-3' for Usp40; F 5'-AAACGCAAACCTTACCAG-3' and R 5'-TATAGGCAGGGCATCAAA-3' for TLR1; F 5'-GTCAGTGCTGGAAATAGAG-3' and R 5'-CACAGGCAGTACATCAAA-3' for TLR6; F 5'- AGGGTGCGGTACACTAAC-3' and R 5'- CAACACGGTATGACAGAAA-3' for MR.

Mouse models

For the iH37Rv-primed mouse model, the μMT (B cell-deficient) mice were intravenously (*i.v.*) injected with ManLAM-treated WT/IL-$10^{-/-}$ B cells on day -3 (5×10^6/100 μl PBS/mouse). On day 0, the mice were immunized (*i. p.*) with iH37Rv (1×10^8 CFU/mouse). On day 7, intracellular IFN-γ, IL-4 and IL-17A production by splenic $CD4^+$ T cells was analyzed by FCM.

WT (C57BL/6J) mice were infected (*i.p.*) with BCG/BCGΔ2196 (1×10^8 CFU/mouse), and splenic B10 cells were determined by FCM at day 20 post-infection. $Rag2^{-/-}$ mice, which have no mature B and T cells, were *i.v.* injected with ManLAM-treated WT/IL-$10^{-/-}$ B cells plus $CD4^+$ T cells (5×10^6 B cells+5×10^6 T cells /100 μl PBS/mouse) at day -7. At day 0, these $Rag2^{-/-}$ mice were *i. v.* infected with BCG (1×10^5 CFU/mouse). At day 20 post-infection, splenocytes were collected. B10 cells, intracellular IFN-γ, IL-4, IL-17A and IL-10 production by $CD4^+$ T cells was determined by FCM. Bacterial loads in the spleens of infected mice were assessed as previously described (Pan et al., 2014; Sun et al., 2016).

For *M.tb* H37Rv infection model, $Rag2^{-/-}$ mice were *i.v.* injected with ManLAM-treated WT / IL-$10^{-/-}$ B cells plus $CD4^+$ T cells (5×10^6 B cells+5×10^6 T cells /100 μl PBS/mouse) at day -7. At day 0, the mice were *i. v.* infected with *M.tb* H37Rv (1×10^5 CFU/mouse). After 20 days of infection, *M.tb* H37Rv loads in the lungs and spleens of infected mice were assessed. The mice were sacrificed by carbon dioxide inhalation.

Cytotoxicity assay

To assess ManLAM cytotoxicity, lactate dehydrogenase (LDH) cytotoxicity assay was performed. B cells were incubated with polymyxin B-treated ManLAM (10 ng/ml), ManLAM or iH37Rv (MOI, 1:2) in the IL-2-containing medium for 2-72 h. The

cytotoxicity of ManLAM was determined by measuring the release of cytoplasmic LDH using CytoTox 96 Non-Radioactive Cytotoxicity Assay (Promega, Madison, WI).

Quantification and statistical analysis

Data are presented as mean ± SD and analyzed by GraphPad Prism V 5.00 for Windows (GraphPad Software, San Diego, CA). Statistical significance was determined by Student *t* test or ANOVA followed by Neuman-Keuls post hoc test. *p* value less than 0.05 considered as statistically significant.

Ethics statement

Participation of human subjects was approved by ethics committee of the Wuhan University School of Basic Medical Science and Wuhan Medical Treatment Center (No. 14009), and blood samples were obtained only after informed written consent.

All mouse experiments in this study were carried out in accordance with the recommendations in the Guide for the Care and Use of Laboratory Animals of the National Institutes of Health and Animal Management Regulations of Animal Laboratory Center of Wuhan University. All mouse experiments were approved and supervised by the Institutional Animal Care and Use Committee of Animal Laboratory Center of Wuhan University (No. 2017077, No. 2017095 and No. 2017095-1).

Data and Software Availability

RNA-seq data reported in this study has been submitted to the NCBI SRA: PRJNA505400 (https://submit.ncbi.nlm.nih.gov/subs/sra/).

Supplementary References

Li D, Li Y, Wu X, Li Q, Yu J, Gen J, et al. (2008). Knockdown of Mgat5 inhibits breast cancer cell growth with activation of CD4+ T cells and macrophages. J. Immunol. 180, 3158-3165.

Pan Q, Wang Q, Sun X, Xia X, Wu S, Luo F, et al. (2014). Aptamer against mannose-capped lipoarabinomannan inhibits virulent Mycobacterium tuberculosis infection in mice and rhesus monkeys. Mol. Ther. 22, 940-951.

Sun X, Pan Q, Yuan C, Wang Q, Tang XL, Ding K, et al. (2016). A Single ssDNA Aptamer Binding to Mannose-Capped Lipoarabinomannan of Bacillus Calmette-Guerin Enhances Immunoprotective Effect against Tuberculosis. J. Am. Chem. Soc. 138, 11680-11689.

Tang XL, Wu SM, Xie Y, Song N, Guan Q, Yuan C, et al. (2016). Generation and application of ssDNA aptamers against glycolipid antigen ManLAM of Mycobacterium tuberculosis for TB diagnosis. J. Infect. 72, 573-586.

Tang XL, Zhou YX, Wu SM, Pan Q, Xia B, Zhang XL. (2014). CFP10 and ESAT6 aptamers as effective Mycobacterial antigen diagnostic reagents. J. Infect. 69, 569-580.

Wang J, Vasaikar S, Shi Z, Greer M, Zhang B. (2017). WebGestalt 2017: a more comprehensive, powerful, flexible and interactive gene set enrichment analysis toolkit. Nucleic Acids Res. Jul 3;45(W1):W130-W137.

Yu G, Wang L, Han Y and He Q. (2012). clusterProfiler: an R package for comparing biological themes among gene clusters. OMICS: A Journal of Integrative Biology. 16(5):284-287.

Zhong B, Zhang L, Lei C, Li Y, Mao AP, Yang Y, et al. (2009). The ubiquitin ligase RNF5 regulates antiviral responses by mediating degradation of the adaptor protein

MITA. Immunity 30, 397-407.